

# Surgery and Matter for 3d Theories

---

Shi Cheng<sup>a</sup>

<sup>a</sup>*Department of Physics and Center for Field Theory & Particle Physics, Fudan University, 20005, Songhu Road, 200438 Shanghai, China*

*E-mail:* [mirror2718@gmail.com](mailto:mirror2718@gmail.com)

ABSTRACT: We try to give a geometric construction for 3d  $\mathcal{N} = 2$  gauge theories using three-manifolds and Dehn surgeries. We follow the story that wrapping M5-branes on plumbing three-manifolds leads to 3d theories with mixed Chern-Simons levels. This construction can be decorated by adding non-compact Lagrangian submanifolds in the cotangent bundles of three-manifolds. The M5-branes wrapping on these submanifolds through M-theory/IIB string duality lead to flavor D5-branes that engineer chiral multiplets. In this note, we only consider unknotted matter circles, which are intersections between these non-compact M5-branes and plumbing manifolds. Then various dualities of 3d theories can be interpreted as Kirby moves and equivalent surgeries. We also find the dictionary between geometric structures of three-manifolds and physical aspects of gauge theories.

---

## Contents

<b>1</b>	<b>Introduction</b>	<b>1</b>
<b>2</b>	<b>Charges as winding numbers</b>	<b>4</b>
2.1	Mirror triality and $ST$ -moves	4
2.2	$\beta$ -Kirby moves	5
2.3	$\beta$ -Kirby introduces matters	6
<b>3</b>	<b>M5-branes on Ooguri-Vafa defects</b>	<b>10</b>
3.1	Lagrangian M5-branes	12
3.2	The parallel move of D5-branes	16
3.3	Brane webs on torus	18
3.4	3d theories from Lens spaces	19
<b>4</b>	<b>Surgery circles and matter circles</b>	<b>21</b>
4.1	Dehn surgeries and $ST$ -moves	21
4.2	Images of matter and gauge circles	22
4.3	Matter circles and cobordism	25
4.4	$ST$ -moves as Rolfsen's surgery twist	29
<b>5</b>	<b>Open problems</b>	<b>33</b>
<b>A</b>	<b>Some basics</b>	<b>34</b>
A.1	Lens space	34
A.2	Lagrangian submanifolds	35

---

## 1 Introduction

There are some nice works on 3d  $\mathcal{N} = 2$  gauge theories e.g. [2–10]. However the geometric engineering is still not very well established yet. Brane webs for some examples are known in e.g.[11–13], while at this stage brane webs cannot encode mixed Chern-Simons levels and generic superpotentials. We think three-manifolds are promising because of their fruitful geometric structures and transformations, such as Kirby moves [21]. We try to propose a new construction based on Dehn surgeries in complement with DGG/GPV construction inspired by 3d-3d correspondence [14–17]. Basically, surgery construction is the compactification of 6d  $(2, 0)$  theories on three-manifolds. Putting M5-branes on some three-manifolds such as Lens spaces leads to 3d  $\mathcal{N} = 2$  gauge theories. M5-branes can also wrap generic three-manifolds, such as plumbed manifolds to generate colorful 3d theories. In recent years, there are many attentions on computing the WRT invariants of plumbed

manifolds [15, 18, 19]. On the physical side, linking numbers of these plumbed manifolds are interpreted as the mixed Chern-Simons levels of 3d theories [20]. In our previous work [1], we extend this story by introducing chiral multiplets and gauging basic mirror dualities. To describe these introduced matter fields, we found plumbing graphs should be extended by adding gray boxes to denote chiral multiplets, as shown in the example in Figure 2. We also found that in the presence of these new objects, some physical dualities match with the first type Kirby moves for three-manifolds. This implies that the introduced gray boxes are compulsory and realistic, and hence should have geometric interpretations. However, in [1], the existence of gray boxes (matter nodes) on three-manifolds is a conjecture. In this note, we confirm this conjecture by exploring the geometric engineering of matters, and find these matters/gray boxes should correspond to Ooguri-Vafa defects given by wrapping M5-branes on Lagrangian submanifolds in the cotangent bundle of three-manifolds.

In practice, finding the geometric correspondences of matters is not easy for us. We firstly notice that the charges of chiral multiplets under gauge groups should be interpreted as winding numbers. This can be known by analyzing Kirby moves and in particular the handle-slides of surgery circles [21]. This step is helpful to interpret geometric transformations as physical dualities, such as  $ST$ -moves (gauged mirror duality) [1]. Because of that, one can conjecture that geometric objects that have winding numbers and engineer matters should be some loops. We use the M-theory/IIB string dualities to figure out that some Lagrangian submanifolds satisfy this property, which are indeed the Ooguri-Vafa's constructions of Wilson loops in [22] by introducing Lagrangian M5-branes to intersect the three-sphere along knots  $L_K \cap S^3 = K$ . In our context, these Ooguri-Vafa defects intersect three-manifolds along some unknots  $L_{\bigcirc} \cap M_3 = \bigcirc$ , which characterize chiral multiplets and hence we call them matter circles. These defects can be checked and confirmed by dualing M5-brane webs to 3d brane webs in IIB string theory. The defect M5-brane is then dual to the D5-brane, which is already known to engineer the flavor symmetry of chiral multiplets, and open strings between D3-brane and D5-brane provide chiral multiplets. Moreover, there are various ways to put these matter circles on a three-manifold  $M_3$ , which engineer chiral multiplets of charges  $q_i$  under the  $i$ -th gauge group  $U(1)_i$ . To see how these circles tangle with three-manifolds, Dehn surgeries have to be considered as all closed orientable three-manifolds can be obtained by Dehn surgeries along links of circles. These surgery circles give gauge groups  $U(1) \times \cdots \times U(1)$ , and hence we call them gauge circles. Matter circles should link to these gauge circles, otherwise matters are decoupled. We notice that Lens space  $L(\pm 1, 1)$  with an OV-defect is special if considering  $ST$ -moves, which is fine as Kirby moves can always represent three-manifolds as surgeries along links with each component has  $\pm 1$  framing numbers.

Many steps need to be done to find the dictionary between three-manifolds and 3d gauge theories, and the geometric realization of matters reveals a more complete construction of 3d theories. In short, Ooguri-Vafa defects that give flavor symmetries should be combined with the Dehn surgeries of three-manifolds. We illustrate the surgery method in Figure 1 and summarize the dictionary in Table 1. The left graph shows the Dehn surgery of three-manifolds  $M_3$ , which is defined by drilling out the neighborhood of a knot  $K$ , and then a solid torus is filled in. The right graph shows that the OV defect  $L$  can be

three-manifolds	plumbing graphs	abelian gauge theories
matter circle $\circ$	$\blacksquare$	chiral multiplet $\mathbf{F}$
gauge (surgery) circle $\bigcirc$	$\bullet_{k_i}$	gauge group $U(1)_{k_i}$
winding num. between $\circ$ and $\bigcirc$	$\bullet \xrightarrow{q_i} \blacksquare$	charge $q_i$ in fund. rep.
linking num. between $\bigcirc$ and $\bigcirc$	$\bullet \xrightarrow{k_{ij}} \bullet$	effective CS levels $k_{ij}$
$\alpha$ -Kirby moves on $\bigcirc$	blow up/down of $\bullet_k$	integrate in/out $U(1)_k$
Rolfsen's twist (4.26)	$ST$ -moves (4.27)	gauged mirror triality
handle-slides of $\circ$ (4.31)	add $\blacksquare$	add chiral multiplets

**Table 1.** The dictionary between three-manifolds, plumbing graphs (which can be viewed as quiver diagrams), and gauge theories.

introduced through the solid torus. When this solid torus is glued back to form the closed three-manifold  $M_3$ , flavor symmetry is introduced and the chiral multiplet is geometrically realized. It is convenient to use plumbing graphs (which are certain quiver diagrams) to

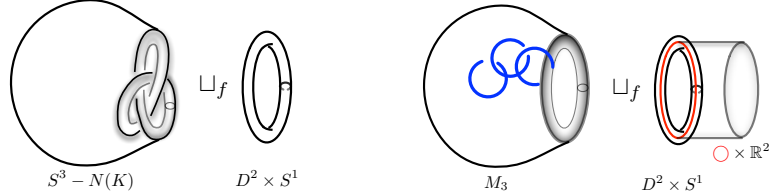


**Figure 1.** Left graph is the surgery construction of three-manifolds. Right graph shows the surgery construction of the 3d theories with matters.

represent 3d theories given by three-manifolds and defects. We illustrate an example in Figure 2. The main ingredients that we introduce are the non-compact defects on the cotangent bundle  $T^*M_3$ . The three-manifold is given by Dehn surgeries along a link of gauge circles, namely  $M_3 = (S^3 \setminus N(\bigcirc_i)) \cup_{f_i} (D_2 \times S^1)_i$  where we have filled in solid tori to make it compact and hence  $\partial M_3 = \emptyset$ .

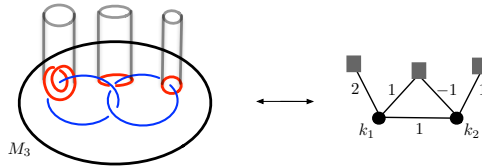


**Figure 2.** Blue circles  $\bigcirc$  are gauge circles for surgeries. Gray tubes denote Lagrangian defects  $L \subset T^*M_3$ . Red circles  $\circ$  as intersections of defects with  $M_3$  are matter circles. This combined geometry corresponds to a 3d theory with gauge group  $U(1)_{k_1} \times U(1)_{k_2}$  and three chiral multiplets  $\Phi_i$  with charges  $(q_i^1, q_i^2)$ . One can represent this theory by its plumbing graph.

In section 2 we show that the winding numbers between matter and gauge circles can be interpreted as charges by considering the handle-slide operation which is the second type of Kirby moves. In section 3 we use M-theory/IIB string duality and brane webs to

show that Lagrangian defect M5-branes along matter circles are dual to D5-branes, and hence engineer chiral multiplets. In section 4 we discuss the locations of matter circles and gauge circles on plumbing three-manifolds given by Dehn surgeries. We will also give a geometric derivation of  $ST$ -moves, in which we use the identical surgery and Rolfsen's rational equivalent twists.

## 2 Charges as winding numbers

In this section, we briefly review the  $ST$ -moves, and discuss another type of Kirby moves — handle-slides that have not been extensively considered in physical literature. We found that handle-slides can be used as a geometric operation to introduce matter nodes on plumbing graphs, and the charges of matters can be interpreted as winding numbers. This implies that matter nodes can be viewed as some kinds of circles, which motivates us to find their geometric realizations. This section is the background for some other sections.

### 2.1 Mirror triality and $ST$ -moves

Let us present what we already know about 3d gauge theories. A well know duality is the mirror duality between a free chiral multiplet and a  $U(1)$  theory with a charge-1 fundamental chiral multiplet:

$$1\mathbf{F} \longleftrightarrow U(1)_{\pm\frac{1}{2}} + 1\mathbf{F}. \quad (2.1)$$

It is convenient to use plumbing graphs to denote this duality:



$$\blacksquare \longleftrightarrow \begin{array}{c} \blacksquare \\ | \\ \bullet \\ \pm\frac{1}{2} \end{array} \quad (2.2)$$

where the numbers  $\pm 1/2$  are bare Chern-Simons levels. This duality is found in [14] by decoupling the antifundamental matter  $1\mathbf{AF}$  in the  $\mathcal{N} = 2$  representation of the basic  $\mathcal{N} = 4$  dual pair:

$$1\mathbf{F} + 1\mathbf{AF} \longleftrightarrow U(1)_0 + 1\mathbf{F} + 1\mathbf{AF}. \quad (2.3)$$

It is noticed and extensively used in [1, 23] that after gauging the  $U(1)$  global symmetry on both sides of (2.1), a new duality is obtained:



$$\begin{array}{c} \blacksquare \\ | \\ \bullet \\ q \\ k \end{array} \xrightarrow{ST} \begin{array}{c} \blacksquare \\ | \\ \bullet \\ +1 \\ \bullet \\ \pm q \\ \bullet \\ k \pm \frac{q^2}{2} \\ \bullet \\ \pm\frac{1}{2} \end{array}, \quad (2.4)$$

where  $q$  is the charge of the matter under the gauge group. The mirror duality (2.1) corresponds to the transformation  $ST \in SL(2, \mathbb{Z})$  in [24] and hence the gauged version (2.4) is called  $ST$ -move. We can use plumbing graphs to denote this gauged duality; see Table 1 for details. Note that in (2.4), we have assigned the bare Chern-Simons levels.

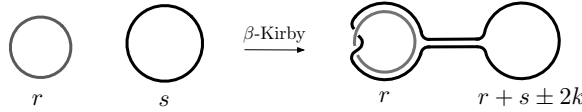
In the following sections, we will only use the effective Chern-Simons levels which receive corrections from chiral multiplets by the formula [2]:

$$k^{\text{eff}} = k^{\text{bare}} + \sum_{I=1}^{N_f} \frac{q_I^2}{2} \text{sign}(q_I) \text{sign}(m_I). \quad (2.5)$$

## 2.2 $\beta$ -Kirby moves

Any three-manifold can be obtained by Dehn surgeries on links, such as the one in Figure 2. However, the links for surgeries are not unique, and there are equivalent surgeries related by Kirby moves which do not change three-manifolds but change the links for surgeries [21], so Kirby moves are geometrically equivalent transformations. Kirby moves contains two types, which are often called first type and second type, or blow-up/down and handle slides. We call them  $\alpha$ -type and  $\beta$ -type in this note<sup>1</sup>. The  $\alpha$ -type is discussed in [1, 20]. Basically,  $\alpha$ -Kirby moves are blow up(down) that introduce(reduce) black nodes on plumbing graphs, which can be interpreted as integrating in(out) gauge groups from physical perspectives. What is interesting is that  $ST$ -move reduces to a particular  $\alpha$ -Kirby move if the matter node is decoupled. However, generic  $\alpha$ -Kirby moves do not perserve if matter nodes are present.

The  $\beta$ -type of Kirby moves is known to be the handle-slide. In literature [21],  $\beta$ -type Kirby move is the operation of linear recombining some components of the links for Dehn surgeries, which can be illustrated in the graph below



$$(2.6)$$

Let us use  $L_1$  and  $L_2$  to denote these two surgery circles, whose framing numbers and linking numbers are as follows

$$L_1 \cdot L_1 = r, \quad L_1 \cdot L_2 = L_2 \cdot L_1 = k, \quad L_2 \cdot L_2 = s, \quad (2.7)$$

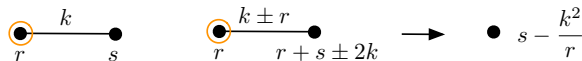
although we did not draw the linking between  $L_1$  and  $L_2$  in (2.6) for simplicity.

After  $\beta$ -type Kirby move, the circle  $L_1$  is unchanged  $\tilde{L}_1 = L_1$ , and  $L_2$  combines with  $L_1$  to form a new circle  $\tilde{L}_2 = L_2 \pm L_1$ . Using (2.7), one can compute new linking numbers:

$$\tilde{L}_1 \cdot \tilde{L}_1 = r, \quad \tilde{L}_1 \cdot \tilde{L}_2 = \tilde{L}_2 \cdot \tilde{L}_1 = k \pm r, \quad \tilde{L}_2 \cdot \tilde{L}_2 = r + s \pm 2k. \quad (2.8)$$

These changes are assigned on the graph (2.6).

It is hard to physically understand this type of Kirby moves, although it can be checked by integrating out the gauge node  $U(1)_r$ , and then the two graphs in (2.6) become the same one:



$$(2.9)$$

<sup>1</sup>In literature e.g.[21], the first type is called  $\kappa$ -move.

This  $\beta$ -Kirby move has some overlaps with but not fully equivalent to  $\alpha$ -Kirby move, since  $\alpha$ -Kirby moves add or reduce gauge nodes, while  $\beta$ -Kirby moves preserve the number of gauge nodes.

One can form other recombinations of circles. It is easy to find that  $\tilde{L}_2 = L_2 + nL_1$  with  $n \in \mathbb{Z}$  could also reduce to the node  $U(1)_{s - \frac{k^2}{r}}$  by integrating out  $U(1)_r$ . This gives a more generic version of  $\beta$ -Kirby moves:

$$\begin{array}{ccc} \bullet_r & \xrightarrow{k} & \bullet_s \\ & & \bullet_r \xrightarrow{k+nr} \bullet_{n^2r+s+2nk} \end{array} \quad (2.10)$$

From another perspective, this move can be viewed as iteratively applying  $n$  times of the  $\beta$ -Kirby move in (2.6). Note that the reverse process is also a  $\beta$ -Kirby move, as  $n$  can be negative integers.

There is a special case that when  $k = 0$  and  $n = 1$ ,  $\alpha$ -Kirby move and  $\beta$ -Kirby move are equivalent  $K_\alpha \simeq K_\beta$ :

$$\begin{array}{ccc} \bullet_r & & \bullet_s \\ & \xrightarrow{nr} & \bullet_r \xrightarrow{nr} \bullet_{s+n^2r} \end{array} \quad (2.11)$$

since in this case, the  $\bullet_r$  is disconnected. In this case, one should set  $r = \pm 1$ , as connecting a three-sphere  $S^3$  to the three-manifold  $M_3$  is always equivalent to itself, namely  $S^3 \# M_3 = M_3$ .

### 2.3 $\beta$ -Kirby introduces matters

For the  $\beta$ -Kirby move in (2.10), the surgery cycle  $L_1$  is not affected, while  $L_2$  changes significantly. However, it is safe to attach a matter to  $L_2$  rather than  $L_1$ , as  $L_1$  can be integrated out as in (2.9).

The non-trivial case is to put a matter node on  $L_1$ :

$$\begin{array}{ccc} \blacksquare & & \blacksquare \\ | & & | \\ \bullet_r & \xrightarrow{k} & \bullet_r \\ & & \bullet_s \end{array} \xrightarrow{\beta\text{-Kirby}} \begin{array}{ccc} \bullet_r & \xrightarrow{k \pm r} & \bullet_{r+s \pm 2k} \\ & & \blacksquare \end{array} \quad (2.12)$$

It is not obvious if this is an equivalent operation. We will give an example soon to show this is not an equivalence.

One can use  $ST$ -moves to understand this case. Let us recall the basic  $ST$ -move:

$$\begin{array}{ccc} \blacksquare & \xrightarrow{ST_\alpha} & \blacksquare \\ | & & | \\ \bullet_k & & \bullet_{k \pm 1} \end{array} \quad (2.13)$$

where we have assigned effective Chern-Simons levels<sup>2</sup>. Since  $ST$ -move reduces to  $\alpha$ -Kirby move after decoupling the matter node, we can figure out how it changes the surgeries circles:

$$\{L_1\} \xrightarrow{ST_\alpha} \{L_1 + L, L\}, \quad (2.14)$$

<sup>2</sup>If we use bare Chern-Simons levels as in (2.4), we can perform  $ST$ -moves many times; see [1] for more details.

for which  $\{L^2 = \pm 1, L_1^2 = k, L \cdot L_1 = 0\}$ . An interesting point is that after the  $ST_\alpha$ -move, the matter node  $\blacksquare$  moves from the circle  $L_1$  to the circle  $L$ .

The surgery circles can also recombine in the same way as the  $\beta$ -Kirby move in (2.10), which defines a  $ST_\beta$ -move:

$$\begin{array}{ccc}
 \begin{array}{c} \blacksquare \\ | \\ \bullet \\ +1 \end{array} & \bullet & \xrightarrow{ST_\beta} & \begin{array}{c} \blacksquare \\ | \\ \bullet \\ +1 \end{array} \text{---} \begin{array}{c} \bullet \\ k+1 \end{array} \\
 & k & & 
 \end{array} \tag{2.15}$$

which is a special  $\beta$ -Kirby move with  $\{r = 1, n = 1\}$  if ignoring the matter node. Here  $r$  can also be  $-1$ , then it corresponds to the  $(ST)^2$ -move<sup>3</sup>. The circles under  $\beta$ -Kirby move change:

$$\{L, L_1\} \xrightarrow{ST_\beta} \{L, L + L_1\}, \tag{2.16}$$

with  $\{L^2 = +1, L_1^2 = k, L \cdot L_1 = 0\}$ . In the  $ST_\beta$ -move, the matter node is always on  $L$ .

The  $ST_\beta$ -move is a special case of (2.12). By combining (2.13) and (2.15), one can see that  $ST_\beta$ -move is not an equivalent operation, since  $\bullet_{+1} - \blacksquare \neq \bullet_k - \blacksquare$ . Although in the absence of matter nodes,  $\beta$ -Kirby moves are equivalent operations. Note that when the matter is very massive and decoupled,  $ST_\beta$ -move reduces to a  $\beta$ -Kirby move. This  $ST_\beta$ -move seems weird, as the decorated node  $\bullet_{+1} - \blacksquare$  on the left graph is disconnected to  $\bullet_k$ , while this decorated node links to  $\bullet_{k+1}$  on the right graph in (2.15). Therefore, we think the  $ST_\beta$ -move is an operation of adding matter nodes to 3-manifold by the connected sum. In short,  $ST_\beta$  is not an equivalent operation, and hence not a duality, while  $ST_\alpha$ -move is a duality.

A naive observation is that one can combine  $ST_\alpha$  and  $ST_\beta$ , which is an operation of sliding (introducing) a matter node  $\blacksquare$  from  $\bullet_{+1}$  to the gauge node  $\bullet_k$ :

$$\begin{array}{ccc}
 \begin{array}{c} \blacksquare \\ | \\ \bullet \\ +1 \end{array} & \bullet & \xrightarrow{ST_\beta \cdot ST_\alpha^{-1}} & \begin{array}{c} \blacksquare \\ | \\ \bullet \\ k \end{array} \\
 & k & & 
 \end{array} \tag{2.17}$$

Geometrically, this combined operation changes the position of the matter node from  $\bullet_{+1}$  to  $\bullet_k$ . So this operation can be used to add matter node  $\blacksquare$  to any gauge node  $\bullet_k$  rather than just  $\bullet_{\pm 1}$ . Note that when the matter node is introduced, the bare CS level  $k$  should be viewed as an effective CS level, so correspondingly the bare CS level shifts from  $k$  to  $k \pm 1/2$ .

Moreover, the matter with charge  $q$  can also be introduced by applying the  $ST_\beta$ -move  $q$  times. Let us consider the  $(ST_\beta)^q$ -move, which combines surgery circles as follows

$$\tilde{L} = L, \quad \tilde{L}_1 = L_1 + qL, \tag{2.18}$$

<sup>3</sup>which means the reverse of  $ST$ , as  $(ST)^{-1} = (ST)^2$  and  $(ST)^3 = 1$ . Notice that for  $r = \pm 1$ , the decorated gauge node is  $\bullet_{\pm 1/2} - \blacksquare$ . Depending on the signs of mass parameters, one can get effective CS levels  $k^{\text{eff}} = \pm 1$  using the formula (2.5).

whose linking numbers are  $\{L \cdot L = +1, \tilde{L} \cdot \tilde{L}_1 = q, \tilde{L}_1 \cdot \tilde{L}_1 = k + q^2\}$ . If an external gauge node (circle)  $L_2$ , namely  $\bullet_g$ , joins in, plumbing graphs change as follows<sup>4</sup>:

$$(2.19)$$

Setting  $a = 0$  and  $b = 0$  could remove the external node and reduces the above graph to an effective version of the  $ST_\alpha$ -move in (2.4)<sup>5</sup>:

$$(2.20)$$

Combining (2.19) and (2.20), one can see that  $(ST_\beta)^q$  introduces a charge  $q$  matter to the gauge node  $\bullet_k$ :

$$(2.21)$$

This charge  $q$  is the multiple number of the circle  $L$  as  $\tilde{L}_1 = L_1 + qL$ , and is also the linking number between  $\tilde{L}$  and  $\tilde{L}_1$ , since  $\tilde{L} \cdot \tilde{L}_1 = q$ .

One can also couple the matter node to many gauge nodes to form a multiple charged matter with the charge  $q_i$  under each  $U(1)_{k_i}$ . For instance, a bifundamental matter can be introduced by  $ST_\beta$ -moves

$$(2.22)$$

where we have assigned effective CS levels. The recombined circles are

$$\tilde{L} = L, \quad \tilde{L}_1 = L_1 + q_1 L, \quad \tilde{L}_2 = L_2 + q_2 L. \quad (2.23)$$

In addition, one can add many matter nodes using  $ST_\beta$ -moves.

From the above examples in this section, one can see that both types of Kirby moves have physical interpretations. One can conjecture that the matter node should be some kinds of circles on three-manifolds, because the charge  $q_i$  is surprisingly interpreted as the winding numbers between the matter and the gauge circle  $\bullet_{k_i}$ . Since the matter node  $\blacksquare$

<sup>4</sup>Decoupling the matter node  $\blacksquare$  and integrating out  $\bullet_{+1}$  and  $\bullet_g$  on both graphs lead to the same gauge node  $\bullet_{k+b^2/(a^2-g)}$ .

<sup>5</sup>In the following parts of this note, we only discuss  $\bullet_{+1} - \blacksquare$ . One can also consider  $\bullet_{-1} - \blacksquare$ , which however leads to the same conclusion.

can be viewed as  $\bullet_{\pm 1} - \blacksquare$  through mirror duality (2.2), matter circles can indirectly use this gauge node  $\bullet_{+1}$  to link any other gauge nodes, which is what  $ST_{\beta}$ -moves tell us. In following sections and in particular section 4.4, we will show that matter circles are indeed exist and are geometrically realized by Lagrangian submanifolds and three-manifolds, as is illustrated in Figure 2. This gives a natural interpretation that charge  $q$  is the winding number.

**Bare CS levels for  $ST$ -moves.** In this note, we only consider circles with integral linking numbers, and hence are effective CS levels. However, in gauge theory analysis, one can also use bare CS levels and then take into account the corrections from matters, such as (2.4). At this stage, we do not clearly know how to geometrically describe bare CS levels (bare linking numbers) using surgeries.

The above examples in this section have shown that the handle-slides ( $\beta$ -Kirby moves) work and match with effective CS levels of 3d theories. Both effective version and bare version have benefits and drawbacks. If using bare CS levels, it would be easy to read off the corrections from matters. Another advantage is that the bare version of  $ST$ -moves shown in (2.4) allows us to freely perform  $ST_{\alpha}$ -moves recursively to form the chain  $\bullet_{k\pm q^2/2} - \bullet_{\pm 1} - \cdots - \bullet_{\pm 1} - \blacksquare$ , although finally many  $\bullet_{\pm 1}$  in the chain can be integrated out, and only two types of moves left as shown in (2.4). However, one cannot consistently do this recursion for the effective version shown in (2.20).

**1-form symmetries.** There are 1-form symmetries for 3d theories, such as the related works in e.g. [25, 26]. We do not clearly know how to analyze 1-form symmetries for graphs with matter nodes, so in this section we only compute the 1-form symmetries that can be read off from effective Chern-Simons levels and then clarify that Kirby moves preserve this discrete symmetry.

Using the Smith decomposition, the effective CS levels can be diagonalized

$$K^{\text{eff}} = U\Lambda V, \quad (2.24)$$

where  $\Lambda = \text{diag}(\Lambda_1, \Lambda_2, \cdots, \Lambda_n)$  is the diagonal matrix, and then the 1-form symmetry reads

$$G^1 = \oplus_i \mathbb{Z}_{\Lambda_i}. \quad (2.25)$$

Dualities should preserve 1-form symmetries, but the equivalence of 1-form symmetries does not mean dualities. For the  $\beta$ -Kirby moves in (2.10), one can check that the 1-form symmetry is invariant and is independent of the winding number  $n$ . If  $r = \pm 1$  and for any  $n \in \mathbb{Z}$ , and then  $G^1 = \mathbb{Z} \oplus \mathbb{Z}_{s-k^2}$ , which is consistent with (2.9). The handle-slide of plumbing graph in (2.21) gives  $G^1 = \mathbb{Z} \oplus \mathbb{Z}_k$  where the  $\mathbb{Z}$  is from  $\bullet_{+1}$ . Note that when  $r = \pm 1$ ,  $\alpha$ -Kirby moves and  $\beta$ -Kirby moves are equivalent, which means that a circle with framing number  $\pm 1$  can be freely removed from plumbing graphs and  $G^1$  does not change. In addition, for the  $\beta$ -Kirby moves (2.10), if  $r = 0, k = 0$ , then  $G^1 = \mathbb{Z}_s$ , and similarly if  $s = 0, k = 0$ , then  $G^1 = \mathbb{Z}_r$ .

From the above computations, we can draw the following conclusion that if the matter is not present, then both the  $\alpha$ -Kirby moves and generic  $\beta$ -Kirby moves preserve the 1-

form symmetry. For example, one can check that linear combinations of surgery cycles  $\{L_i\} \rightarrow \{\tilde{L}_i\}$  given by handle sliding the node  $\bullet_{\pm 1}$ , such as (2.22) if ignoring the matter node, lead to 1-form symmetries of the form  $\mathbb{Z} \oplus \mathbb{Z}_*$  where the  $\mathbb{Z}$  comes from the gauge node  $\bullet_{\pm 1}$ . Note that the winding numbers  $q_i$  of handle slides do not contribute to the 1-form symmetry.

### 3 M5-branes on Ooguri-Vafa defects

In recent years, there are some promising string compactifications for engineering 3d theories, such as [27–30], and here we propose another one. In this section, we consider M5-branes and 3d brane webs, and show that M5-branes wrapping on the Ooguri-Vafa type of Lagrangian submanifolds in the cotangent bundle of 3-manifolds are dual to D5-branes that engineer flavor symmetries for chiral multiplets.

**Ooguri-Vafa defects.** The M5-brane configuration we mean is the twisted compactification of the 6d (2,0) theories on three-manifolds, which is known to be the DGG/PGV construction [14, 15]. In this note, we only consider abelian theories and hence only a single M5-brane wraps on the three-manifold  $M_3$ .

M5-branes reduce to brane systems in IIA-string theory and then is T-dual to 3d brane webs in IIB-string theory, from which one can identify 3d theories and read off matter content. For instance, the case that wrapping M5-branes on Lens spaces  $L(k, 1)$  has been considered in [15, 20, 33, 34]. However, chiral multiplets associated with matter fields have not been found, and we will solve this problem in this section.

To engineer matters, one can get some hints from the common features. Chiral multiplets and hypermultiplets usually associate with flavor symmetries that are given by non-compact manifolds, so we suspect that matters are related to boundaries, or external non-compact manifolds. Ooguri-Vafa (OV) construction of Wilson loops in Chern-Simons theories is given by Lagrangian M5-branes intersecting with a three-sphere along knots  $L_K \cap S^3 = K$ . Inspired by this, we consider a more simple case that the codimensional-two Lagrangian defect  $L_{\bigcirc}$  that intersects the Lens space along a circle  $L_{\bigcirc} \cap L(k, 1) = \bigcirc$ . To check this candidate, one can put M5-branes on  $L_{\bigcirc}$  and see if everything is consistent with 3d brane webs, since it is already known that fundamental chiral multiplets are given by open strings between D3-branes and D5-branes. We focus on the most simple theory  $\bullet_k - \blacksquare$  (namely  $U(1)_k + 1\mathbf{F}$ ), and discuss its 3-manifold realization and the corresponding 3d brane webs in IIB-string theory; see also e.g. [13, 31, 32].

**Lens spaces in M-theory.** Let us first review the Lens spaces in the spacetime of M-theory to have a background. The 11-dimensional spacetime of M-theory is

$$\mathbb{R}_\epsilon^2 \times S^1 \times T^*L(k, 1) \times \mathbb{R}^2, \quad (3.1)$$

where the 3d theories is on the spacetime  $\mathbb{R}_\epsilon^2 \times S^1$  and  $\epsilon$  is the Omega deformation parameter that can be viewed as the mass parameter for the adjoint chiral matter that descends from the vector multiplet in 3d  $\mathcal{N} = 4$  theories.  $T^*L(k, 1)$  is the cotangent bundle  $N \hookrightarrow$

$T^*L(k, 1) \rightarrow L(k, 1)$  with  $N = \mathbb{R}^3$  as the fiber. The special direction is the 11-th direction that arises in the strong coupling limit of IIA string theory, namely M-theory/ $S_{\sharp}^1 = \text{IIA}$ . In this spacetime, we should set  $S_{\sharp}^1 \subset L(k, 1)$ , since Lens spaces have the nice property that they can be obtained by gluing the boundary tori of two solid tori  $D^1 \times S^1$ . If we rewrite  $D^2 = S^1 \times I$ , then Lens spaces are realized as torus bundles over the interval  $I$ , namely  $T^2 \hookrightarrow L(k, 1) \rightarrow I$ , where on each endpoint of the interval  $I$ , the meridian of a solid torus shrinks and only the longitude  $S^1 = \{*\} \times S^1 \in D^2 \times S^1$  survives. In particular, for the Lens space  $L(0, 1) = S^2 \times S^1 = T^2 \times I$ , the survived longitudes at both endpoints are the same.

The theories with a gauge group  $U(N_c)_k$  are given by wrapping  $N_c$  M5-branes on  $\mathbb{R}_c^2 \times S^1 \times L(k, 1)$ . The rotation symmetry on the fiber encodes the R-symmetry  $U(1)_R$  of 3d  $\mathcal{N} = 2$  theories. In this note, we set  $N_c = 1$  and only wrap a single M5-brane on three-manifolds to engineer abelian theories. The Lagrangian defect  $L_{\circ}$  should extend in the fiber of  $T^*L(k, 1)$ , and intersects the base Lens space along a circle, namely  $L_{\circ} = \mathbb{R}^2 \times \circ \subset T^*L(k, 1)$  with  $\mathbb{R}^2 \subset N$  and  $\circ \subset L(k, 1)$ . Since cotangent bundles of three-manifolds are always trivial vector bundles, there is no need to worry if there are different shapes for the  $L_{\circ}$  in the fiber<sup>6</sup>.

We found in this section that the possible position of defects can be illustrated by Figure 3, in which the gauge group is realized by a M5-brane wrapping on the whole Lens space. The gauge group is  $U(1)_k$  and the defect M5-brane leads to a fundamental matter with the flavor symmetry  $U(1)_F$ . In this figure, we put the defect M5-brane on the left endpoint, which could move parallelly to the right endpoint; see Figure 4. In addition, the red circle as the intersection is named as the matter circle.

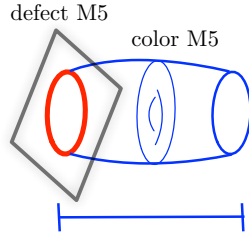


**Figure 3.** The Lens space  $L(k, 1)$  is the torus bundle fibered over an interval. Each half of this bundle is a solid torus.

**M-theory/IIB duality.** It is not obvious how the matter circles  $\circ$  intersects Lens spaces if not considering string dualities. Let us recall the duality between M-theory and IIB string theory. This duality applies on the spacetime

$$\mathbb{R}_{12}^2 \times S_0^1 \times N_{345} \times L(k, 1)_{69\sharp} \times \mathbb{R}_{78}^2, \quad (3.2)$$

where we have assigned coordinates on all directions. The elliptic fiber bundle reads  $T_{9\sharp}^2 \hookrightarrow L(k, 1) \rightarrow I_6$ , where the torus fiber  $T_{9\sharp}^2 = S_9^1 \times S_{\sharp}^1$  has longitude  $S_9^1$  and meridian  $S_{\sharp}^1$ . We

<sup>6</sup>We would like to thank Kewei Li for discussion on this point.

remind that the identification of meridian and longitude is important, and they cannot be switched freely.

The M/IIB duality is a combination of T-duality and S-duality in string theories. Basically, the T-duality is the process of shrinking some directions on Dp-branes:

$$\text{Dp wrap on } x_i \xleftarrow{\text{T-dual on } x_i} \text{D}(p-1) \text{ at a point on } x_i, \quad (3.3)$$

where  $x_i$  is a direction that Dp-brane extends on. The M-theory and IIB string theory are related through the torus  $M/T_{9\sharp}^2 \simeq \text{IIB}/S_9^1$ . More specifically,

$$\text{M-theory} \xrightarrow{\text{shrink } S_{\sharp}^1} \text{IIA} \xrightarrow{\text{T-dual along } x^9} \text{IIB}. \quad (3.4)$$

In addition, because of the relation

$$\frac{l_p^3}{R_9 R_{\sharp}} = \tilde{R}_9, \quad (3.5)$$

the radius of the dual circle in IIB is infinitely large  $\tilde{R}_9^1 \rightarrow \infty$ , as the area of the the torus vanishes at both endpoints of the interval  $I_6$ , namely  $R_9 R_{\sharp} \rightarrow 0$ .

### 3.1 Lagrangian M5-branes

As discussed in [31], M5-branes are dual to  $(p, q)$ 5-branes in IIB string theory, depending on the winding numbers of the M5-brane along  $S_{\sharp}^1$  and  $S_9^1$ . These 5-branes locate at endpoints of the interval  $I_6 \in L(k, 1)$  that presents a D3-brane. We fix the brane configuration and present it in Table 2.

In short, we find the Lagrangian defects should wrap the longitude  $S_9^1$  to engineer matters, because only these defect M5-branes are dual to flavor D5-branes, and each defect M5-brane corresponds to a hypermultiplet in fundamental representation, which contains two chiral matters with opposite charges  $\pm q$ . Interestingly, we notice that the winding number of the defect M5-brane along  $S_9^1$  is the charge  $q$  of the chiral multiplet, which matches with the conjecture we draw in section 2.3. In the following, we show some details.

**From Lens spaces to 3d brane webs.** To begin with, the gauge group is engineered by a single M5-brane wrapping on the whole Lens space  $L(k, 1)$ . It reduces to a D4-brane after shrinking the 11-th circle  $S_{\sharp}^1$ , and then T-duality along the meridian  $S_9^1$  of the torus  $T_{9\sharp}^2$  turns it into a D3-brane in IIB string theory, which gives rise to a gauge group  $U(1)$ . In short,  $M5(1269\sharp) \rightarrow D4(1269) \rightarrow D3(126)$ . This process is present in Table 2.

The bare CS level of this gauge group  $U(1)_k$  is determined by the relative angle  $\theta$  between two NS5-branes. These NS5-branes comes from the reduction of D6-branes on two endpoints of the interval  $I_6 \in L(k, 1)$ , which are magnetic monopoles of D0-branes that are Kaluza-Klein modes of the graviton along  $S_{\sharp}^1$ , and hence D6-branes emerge only at points where the  $S_{\sharp}^1$  shrinks. For Lens spaces, only at the endpoints of the interval  $I_6$ ,  $S_{\sharp}^1$  shrinks and hence D6-branes emerge; see e.g.[33] for more discussions. The D6-brane is T-dual to a D5-brane in IIB string theory. For a gauge theory, what we want to produce is a

		$S^1 \times \mathbb{R}^2$			$N_{345}$			$I_6 \times T_{9\#}^2$			$\mathbb{R}^2$	
11d	branes	0	1	2	3	4	5	6	9	#	7	8
M-theory	$N_c$ M5	0	1	2				6	9 <sub>A</sub>	#		
IIA	$N_c$ D4	0	1	2				6	9 <sub>A</sub>			
IIB	$N_c$ D3	0	1	2				6				
IIA	D0									#		
IIA	D6	0	1	2	3	4	5		9 <sub>A</sub>			
IIB	D5 $\xrightarrow{S}$ NS5	0	1	2	3	4	5					
M-theory	M5''	0	1	2	3	4			9 <sub>A</sub>			
IIA	NS5''	0	1	2	3	4			9 <sub>A</sub>			
IIB	NS5'' $\xrightarrow{S}$ D5	0	1	2	3	4			9 <sub>B</sub>			
M-theory	M2	0					5		9 <sub>A</sub>			
IIB	D1 $\xrightarrow{S}$ F1	0					5					
M-theory	M5'	0	1	2	3	4				#		
IIA	D4'	0	1	2	3	4						
IIB	D5' $\xrightarrow{S}$ NS5	0	1	2	3	4			9 <sub>B</sub>			
M-theory	M2	0					5			#		
IIB	F1 $\xrightarrow{S}$ D1	0					5					

**Table 2.** In this table, we show related branes and their directions at one endpoint of the interval  $I_6$ . Since the direction  $x_9$  appears in both IIA and IIB, we use a subscript in  $9_A$  and  $9_B$  to distinguish. In this table, we use different colors to emphasize some branes. The branes on the other endpoint can be obtained by shifting coordinates through gluing maps.

NS5-brane, so the S-duality in IIB should be applied to turn D5-brane into NS5-brane. In short, the process of obtaining NS5-branes is  $D0 \rightarrow D6(\text{IIA}) \rightarrow D5(\text{IIB}) \xrightarrow{S} \text{NS5}(\text{IIB})$ . At the other endpoint of  $I_6$ , another NS5'-brane is emerged, which differs from the NS5 by a relative angle  $\theta$ , and the Chern-Simons level yields  $k = \tan \theta$ , which is the framing number of  $L(k, 1)$ .

The above construction gives the 3d brane web NS5 – D3 – NS5'. We need to compare various brane configurations in [31] to see if the above construction through Lens space is allowed. In [31], there are three ways to break  $\mathcal{N} = 4$  to  $\mathcal{N} = 2$  by turning on various relative angles. Fortunately, the 3d brane web we just obtained is one of them, which is the case that requires the condition  $\rho = \theta$ , where  $\rho$  and  $\theta$  are the relative angles on planes  $x_{9\#}$  and  $x_{59}$  respectively. Because of this particular condition, there is no much difference between NS5 and D5, as they only differ by an angle on the plane  $x_{59}$ . This special case of 3d brane webs can also be obtained by Higgsing 5d  $\mathcal{N} = 1$  brane webs by conifold transitions; see e.g. [13, 32, 35]. In IIB-string theory, we often set  $\theta = \pi/2$  to distinguish NS5 and D5, which means NS5 is along vertical direction and D5 is along horizontal direction on plane  $x_{59}$ , and the NS5'-brane should be more precisely called  $(k, 1)$  5-brane<sup>7</sup>.

<sup>7</sup>For a  $(p, q)$ -brane,  $p$  is the electric charge and  $q$  is the magnetic charge.

Let us consider the defect M5-brane which in our context is the Lagrangian submanifold of the Ooguri-Vafa type, wrapped by a M5-brane. A M5-brane on  $\mathbb{R}_{45}^2 \times S_9^1 \subset N_{345} \times L(k, 1)_{69\sharp}$  leads to a D5-brane through M/IIB duality and S-duality, as shown in Table 2. This D5-brane is responsible for the flavor symmetry  $U(1)_F$  and introduces a hypermultiplet through the open string between D3 and this D5. For  $L(0, 1)$ , what we get is a  $\mathcal{N} = 4$  theory  $U(1)_0$  with a hypermultiplet. If  $k \neq 0$ , then  $\mathcal{N} = 4$  breaks to  $\mathcal{N} = 2$ , and the hypermultiplet can be viewed as a sum of a fundamental chiral multiplet (**F**) and an antifundamental chiral multiplet (**AF**)<sup>8</sup>. The evolution of the defect brane is

$$M5''(12349) \rightarrow \text{NS5}(12349)(\text{IIA}) \rightarrow \text{NS5}(12349)(\text{IIB}) \xrightarrow{S} \text{D5}(12349)(\text{IIB}).$$

For this defect and Lens space, the intersection is the longitude  $M5 \cap M5'' = S_9^1$ .

**Mass parameters.** The defect M5-brane is suitable for engineering matters, since M2-branes on the defect M5-brane agree with open strings in 3d brane webs. We can try to find the corresponding mass parameters and FI parameters.

Recall that the length of the F1-strings between the D3 and D5 is the real mass parameter, while that of D1-branes between D3 and NS5 is the FI parameter. F1 and D1 can be exchanged through S-duality. Since defect  $M5''$  and bulk M5 are separated along direction  $x_5$ , the M2-brane stretches between these two M5-branes, and one of its boundaries is the intersection  $\partial(M2) = M2 \cap M5 = S_9^1$ , and the other boundary is the intersection  $\partial(M2) = M2 \cap M5'' = S_9^1$ . The M2-brane should be a tube  $I_5 \times S_9^1$  rather than a disc. In short, the M2-brane descends as  $M2(59) \rightarrow D2(59) \xrightarrow{T_9} D1(5) \xrightarrow{S} F1(5)$  under dualities. The mass parameter as the length of  $I_5$  is the coordinate  $m = x_5$  that takes values from  $(-\infty, +\infty)$ , whose sign depends on the orientation. If the matter is massless, then  $m = x_5 = 0$ . Note that when  $S_9^1 \rightarrow 0$ , the matter is also massless. We will revisit mass parameter in section 4.4, in which we will comment that  $S_9^1$  is more suitable for mass parameters for theories given by 3-manifolds.

Moreover, because of the relation (3.5), at a generic point on the interval  $I_6$  the fiber torus has a non-vanishing area. Therefore, the D5-brane introduced by a defect is a loop on  $S_{9_B}^1$  with a finite radius. Only when this defect is moved to endpoints, the radius of this loop becomes infinite large. In this sense, the Lens spaces with Ooguri-Vafa defects match with corresponding 3d brane webs with D5-branes.

One can also consider the defect  $M5'$  along the meridian  $S_{\sharp}^1$ . However, if we perform S-duality, then  $M5'(1234\sharp) \rightarrow D5'(12349) \xrightarrow{S} \text{NS5}(12349)$ , which unfortunately is not a D5 and hence this  $M5'$  is not very suitable for engineering matters, although there is an exception; see (3.9). In this disregarded case, the M2-brane between the bulk M5 and defect  $M5'$  is finally dual to a D1-brane:  $M2(5\sharp) \rightarrow F1(5) \xrightarrow{T_9} F1(5) \xrightarrow{S} D1(5)$ . The topology of this M2-brane is a tube  $I_5 \times S_{\sharp}^1$ , and hence the distance  $I_5$  engineers the FI parameter. Note that at endpoints of  $I_6$ ,  $S_{\sharp}^1$  shrinks and hence FI parameter always vanishes.

---

<sup>8</sup>Note that in plumbing graphs of this note, all **AF** are decoupled, such as (2.4). The matter node  $\blacksquare$  only denotes a fundamental chiral multiplet **F**. We will give more comments on this decoupling in other parts of this note.

**FI parameters.** FI parameter in principle is independent of the defect M5-brane as it is given by the length of the D1-string stretching between D3 and NS5. Unfortunately, we have not successfully identify the FI parameter through M/IIB duality. We will revisit FI parameter in section 4.4, in which we will show that the length of the surgery circle is more suitable for FI parameters for theories given by 3-manifolds.

In below, we show two interesting configurations for M2-branes, which though are appropriate for other physical interpretations. Both candidates suggest  $S_9^1$  is responsible for the FI parameter in other contexts.

In M-theory and topological strings, FI parameter is known as the volume of the M2-brane ending on the bulk M5 in e.g. [22]. For Lens spaces, there is naturally a circle  $S_9^1$  which does not shrinks. For this candidate, the topology of this M2-brane is a disc with  $S_9^1$  as its boundary, and the bulk of M2 extends to the Lens space.

Another configuration is the massless M2-brane taking on  $T_{9\sharp}^2$ , which can be inserted in the worldvolume of the bulk M5-brane. Note that this M2-brane does not have a boundary. However, because of the existence of the D0-brane, there should be a subtle interaction that traps this M2-brane at the volume of the bulk M5-brane. This M2-brane M2(09<sub>A</sub>♯) leads to F1(09<sub>A</sub>) in IIA and then is T-dual to F1(09<sub>B</sub>) in IIB. After S-duality, this F1 turns into a D1(9<sub>B</sub>). Once again, because of the M/IIB duality, the radius of  $S_{9\text{B}}^1$  opens up and becomes infinite large. This D1(9<sub>B</sub>) seems could engineer the FI parameter, because in 3d brane webs, D3 and NS5 locate at two separate points on the direction  $x_{9\text{B}}$  and the distance between them is FI parameter. We can also use IIA to keep track of D3 and NS5. The M5-brane system reduces to D4 – D6 with the intersection being  $S_{9\text{A}}^1$  wrapped by F1(9<sub>A</sub>), namely  $D4 \cap D6 = F1$ . After the T-duality along  $S_{9\text{A}}^1$ ,  $D4 \rightarrow D3$  and  $D6 \rightarrow \text{NS5}$ , and the D3 can be deformed away from NS5 along  $x_{9\text{B}}$ . Note that this F1-string is given by the M2-brane in the volume of M5-brane, so it is a self-dual string.

**Charges and  $(p, q)$ -branes.** In [31], it is discussed that a defect M5-brane can wrap  $q$  times along  $S_9^1$ . This M5-brane is dual to a charge- $q$  NS5-brane, which after S-duality becomes a charge- $q$  D5-brane. The charge- $q$  D5-brane suggests a 3d brane web D3(6)–NS5(5)–D5 <sup>$q$</sup> (9), which engineers a charge- $q$  matter. There are  $q$  Higgs vacua for the D3 to end on the charge- $q$  D5-brane. These  $q$  vacua are points that are evenly distributed on  $S_{\sharp}^1$ , which separate the charge- $q$  D5-branes into  $q$  fractions as shown in Figure 5. The relative real mass parameters between D5-brane fractions are  $m_i \sim S_{\sharp}^1/q$ . Since  $S_{\sharp}^1$  shrinks on endpoints of  $I_6$ , these fractions coincide to an overlapped charge- $q$  D5-branes on endpoints. There is still an overall mass parameter  $m_0$  left, which is the length of the F1(5) string along  $x_5$  that connects D3 and the charge- $q$  D5.

Moreover, if a M2-brane wraps  $q$  times on  $S_9^1$  and  $p$  times on  $S_{\sharp}^1$ , then one can get a  $(p, q)$ -string along  $x_5$  in IIB. Generically, a defect M5-brane wrap a  $(q, p)$  curve on  $T_{9\text{A}\sharp}^2$  leads to a  $(p, q)$ 5-brane along  $x_{12349\text{B}}$ . Once again, this brane configuration shows that the charges should be winding numbers, which agrees with what we have learned from handle slides in section 2.

**Gluing maps.** The bare CS level  $k$  is engineered by the framing number of the Lens

space  $L(k, 1)$ . Its definition is slightly different from linking numbers, which needs the information of gluing maps between two solid tori. We can denote  $S_{\sharp}^1$  and  $S_9^1$  by meridian  $\alpha$  and longitude  $\beta$  for later convenience, as they will be named gauge circle and matter circle respectively. These two circles are transformed by the gluing map which is an element in the mapping class group  $SL(2, \mathbb{Z})$ . The gluing map  $f : T^2 \mapsto T^2$  is represented as a matrix:

$$\begin{bmatrix} \tilde{\alpha} \\ \tilde{\beta} \end{bmatrix} = \begin{bmatrix} k & 1 \\ -1 & 0 \end{bmatrix} \cdot \begin{bmatrix} \alpha \\ \beta \end{bmatrix}. \quad (3.6)$$

The framing number is defined as  $k := \beta \cdot \tilde{\alpha}$ , which is the linking number between the longitude and the deformed meridian. However, in terms of circle/surgery representation of Lens spaces in section 2.3 and in particular handle slides, it is more natural to use the self-intersection notation  $L \cdot L := \beta \cdot \tilde{\beta} = k$ . These two definitions are equivalent, as surgery is gluing back a solid torus to a torus hole (a circle complement), so the meridian and longitude should be switched.

The charge- $q$  matter circle is the connected sum of  $q$  number of the charge-1 matter circle, so it is given by  $\beta_q = q\beta$ . The intersection/linking numbers between the gauge and matter circles only concern the solid torus that is glued in the complement and hence are invariant under different gluing maps, so that  $\alpha_q \cdot \beta = \tilde{\alpha}_q \cdot \tilde{\beta} = q$ , as  $\alpha \cdot \alpha = 0$ ,  $\beta \cdot \beta = 0$ ,  $\alpha \cdot \beta = 1$ .

**3d theory on  $S^1 \times \text{tube}$ .** One can consider a trivial three-manifold  $T^2 \times I$ , where the torus never degenerates on the interval  $I$ . This geometry can be obtained from  $S^2 \times S^1$  by truncating two poles of  $S^2$ . For this geometry, since no  $S^1$  degenerates, one can not get D6-branes. Fortunately, one can add defect M5-branes on meridian and longitudes of  $T^2$  to get NS5-branes and D5-branes respectively. This geometry is useful, as it can be used to connect Lens spaces. We will go back to this geometry in section 4.3.

### 3.2 The parallel move of D5-branes

The move of D5-branes in [13] can be described by gluing maps in (3.6) for Lens spaces, which is the parallel transport of circles from one endpoint to another endpoint of  $I_6$ . Explicitly, the  $S_9^1$  and  $S_{\sharp}^1$  are mapped to  $\tilde{S}_9^1$  and  $\tilde{S}_{\sharp}^1$  where  $\tilde{S}_9^1 = -S_9^1$  and meridian is twisted as  $\tilde{S}_{\sharp}^1 = kS_9^1 + S_{\sharp}^1$ . This implies that the charges of 5-branes are not preserved under parallel movement.

The bulk M5-brane on Lens space  $L(k, 1)$  is dual to the 3d brane web NS5 – D3 –  $(k, 1)$ 5-brane, where NS5 and  $(k, 1)$ 5-brane are differed by a relative angle  $k = \tan \theta$ . The S-duality transforms it to D5 – D3 –  $(1, k)$ 5-brane. Note that instead of generating  $(1, k)$ 5-brane from a D6-brane, it can also arise from a defect M5-brane wrapping  $\tilde{S}_{\sharp}^1 = kS_9^1 + S_{\sharp}^1$ , if we forget some constraints; see Table 2.

The flavor D5 brane given by the defect M5 is almost invariant under the gluing map, as  $\tilde{S}_9^1 = -S_9^1$  only reverses its charge. This means that if we move a D5-brane from one endpoint of  $I_6$  to the other endpoint, we still get the same D5-brane only with its orientation flipped, namely the signs of charges for 3d chiral multiplets are shifted. This is consistent with an already known fact from 3d brane webs in IIB string theory [13]. We use the Figure

4 to illustrate this parallel movement of the defect M5-branes/D5-branes, where the red line (D5-brane) gives a hypermultiplet, or in other words, a pair of chiral multiplets  $1\mathbf{F} + 1\mathbf{AF}$ , which after the mover changes to  $1\mathbf{AF} + 1\mathbf{F}$ .

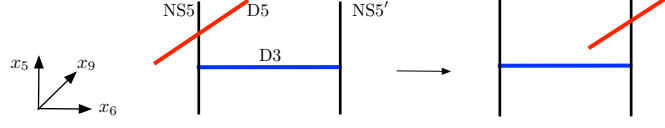


**Figure 4.** The movement of a D5-brane in the 3d brane web. After the movement, the orientation of D5-brane is reversed, which switches the charges of chiral multiplets.

**An exceptional case and decoupling.** Some Lens spaces could engineer abelian 3d  $\mathcal{N} = 4$  theories, as they differ to 3d  $\mathcal{N} = 2$  theories only by turning off Chern-Simons levels. We can let the bare Chern-Simons level vanishing, then  $\text{NS5}' = \text{NS5}$  and the Lens space can only be  $L(0, 1) = S^1 \times S^2$ . In the presence of a D5-brane, we have a hypermultiplet. To get the theory  $\bullet_k - \blacksquare$  with only one  $\blacksquare$ , we should decouple a matter  $\mathbf{AF}$  by sending its mass  $m_a \rightarrow -\infty$ . More explicitly, since the formula for effective Chern-Simons level is  $k_{\text{eff}} = k + (N_f \text{sign}(m_f) - N_a \text{sign}(m_a))/2$  for the theory  $U(1)_0 + N_f \mathbf{F} + N_a \mathbf{AF}$ , one should let two matters in the theory  $U(1)_0 + 1\mathbf{F} + 1\mathbf{AF}$  have opposite signs, namely  $\text{sign}(m_f)\text{sign}(m_a) < 0$ , such that eventually  $k_{\text{eff}} = \pm 1$  to produce the basic building block  $U(1)_{\pm 1} + 1\mathbf{F}$ , which is required for constructing plumbing theories through  $ST$ -moves and Kirby moves. It is already known how to perform decoupling and give opposite signs to both matters on 3d brane webs, while in the M-theory and 3-manifolds it is unclear before.

The patterns of various decoupling are discussed in [13]. In below, we present the 3d brane web for  $U(1)_0 + 1\mathbf{F} + 1\mathbf{AF}$  and its decoupled brane webs for plumbing graph  $\bullet_{+1} - \blacksquare$ . If we look at the brane webs along direction  $x_6$ , they take the following form

(3.7)

where the blue dots are the D3-brane, red lines are D5, and vertical lines are NS5. The 3d brane webs for  $U(1)_{\pm 1}$  with a D5-brane can also reduce to  $\bullet_{\pm 1} - \blacksquare$ . We briefly draw brane webs to illustrate:

(3.8)

The 3d brane web for  $U(1)_{\pm 1}$  with a NS5-defect is a special case that we noticed unexpectedly, as it finally also leads to  $\bullet_{\pm 1} - \blacksquare$ . We illustrate transformations of brane webs below

(3.9)

where from (a) to (b), we apply the S-duality, and from (b) to (c) we just change the slope of (b) using  $SL(2, \mathbb{Z})$  transformation of IIB string theory, which turns  $(p, \pm 1)$ -brane to  $(p + n, \pm 1)$ -brane, but preserves  $(\pm 1, 0)$ -brane. The (c) and its equivalent web (d) are the brane web for the theory  $T[U(1)] + 1D5$ , where  $T[U(N)]$  is the self-dual theory found in [36]. Obviously, if further applying S-duality on (c), one gets the first brane web in (3.7) which is the theory  $U(1)_0 + 1\mathbf{F} + 1\mathbf{A}\mathbf{F}$  and equivalently  $T[U(1)] + 1D5$ . Similarly, one can also draw the brane webs for  $U(1)_{1/n} + 1NS5$  for any  $n \in \mathbb{Z}$ , which always end up with the same web (d) up to the  $SL(2, \mathbb{Z})$  transformation. Thus, this particular theory  $U(1)_{1/n} + 1NS$  with a defect along  $S_{\sharp}^1$  also carries matters, although the defect leads to a NS5. This phenomenon matches with the property that  $L(1, n) = S^3$  for which  $n$  is caused by equivalent twists, and we will discuss this more in the paragraph below (4.10).

### 3.3 Brane webs on torus

In this section, we find it seems possible to put M5-brane webs on torus  $T_{9\sharp}^2$  of M-theory, from which matters with generic charges can be constructed, which however are not known from 3d brane webs in IIB.

**Brane webs on torus.** There are different winding patterns for the defect M5-branes on  $T_{9\sharp}^2$ . We find that on this torus, one can equivalently analyze the dual 3d brane webs, which even suggest new 3d brane webs. Wrapping a defect M5-brane  $q$  times along longitude  $S_9^1$  and  $p$  times along meridian  $S_{\sharp}^1$  leads to a charge  $(p, q)$  5-brane along  $(12349_B)$ , see e.g. [31]. After S-duality in IIB, this 5-brane becomes a  $(q, p)$  5-brane. One can take a quotient  $\mathbb{Z}_q$  on the torus to produce this winding number (charge)  $q$ . We illustrate this in Figure 5. If we put a defect  $(1, 1)$ , then the quotient maps it to  $(q, 1)$ .

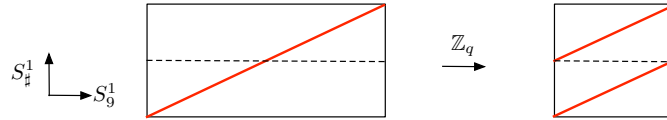


**Figure 5.** In this example we have  $q = 2$ . The charge  $q$  equals to the number of components distributed along meridian  $S_{\sharp}^1$ . The red line is the circle wrapped by the defect M5. The quotient is given by  $S_{\sharp}^1 \rightarrow S_{\sharp}^1$ ,  $S_9^1 \rightarrow qS_9^1$ .

Recall that the D6-brane comes from D0-brane on  $S_{\sharp}^1$ , which can be represented as a vertical line on the torus. A charge  $q$  D5 is given by horizontal lines in (3.10).

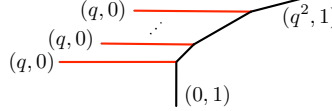
(3.10)

On this torus, the vertical and horizontal lines do not represent the same type of branes, so it is more better to consider the dual brane webs in IIB to see if these lines can be combined into other branes. In the IIB, if a NS5 meets a charge  $q$  D5, then one can split the D5 into two half-infinite lines, and each half-infinite line gives to a chiral multiplet of charge  $q$

or  $-q$ , depending on their positions. If one considers effective CS levels and the fusion of 5-branes, the slope of the parallelly transported NS5 is shifted by the formula (2.5):

$$\Delta k = \tan \theta = \frac{q^2}{2} \text{sign}(m_{\mathbf{F}_q}) - \frac{q^2}{2} \text{sign}(m_{\mathbf{AF}_{-q}}). \quad (3.11)$$

Therefore, every time when a NS5 meets a charge  $q$  component, the merged 5-brane picks up an additional charge  $(q, 0)$  because of the charge conservation. There are  $q$  fractions, and hence the NS5 is finally becomes a  $(q^2, 0)$ -brane<sup>9</sup>:



$$(3.12)$$

In particular,  $\Delta k = \pm q^2$  if  $\text{sign}(m_{\mathbf{F}_q}) \cdot \text{sign}(m_{\mathbf{AF}_{-q}}) = -1$ , and  $\Delta k = 0$  if  $\text{sign}(m_{\mathbf{F}_q}) \cdot \text{sign}(m_{\mathbf{AF}_{-q}}) = +1$ .

We are interested in the Lens space  $L(0, 1)$  with a charge  $q = +1$  matter and  $\Delta\theta = \pm\pi/4$ , as this theory gives to  $\bullet_{+1} - \blacksquare$  after decoupling the  $\mathbf{AF}$  which shifts the slope of NS5 to NS5' as follows:



$$(3.13)$$

Correspondingly, the slope of the shrinking circle  $S_{\sharp}^1$  wrapped by D0 should also be shifted from  $S_{\sharp}^1 \rightarrow S_{\sharp}^1 \pm S_0^1$ ; then this quantum correction transforms  $L(0, 1)$  into  $L(\pm 1, 1)$ . It is a geometric transformation when a defect M5 (denoted as  $L_{\circ}$ ) is present:

$$S^1 \times S^2 \sqcup \tilde{L}_{\circ} \xrightarrow{\text{decoupling } \mathbf{AF}} S^3 \sqcup L_{\circ}, \quad (3.14)$$

which gives effective CS levels  $k_{\text{eff}} = \pm 1$ . Moreover, instead of decoupling both chiral multiplets, we can also decouple  $\mathbf{AF}$  by taking  $m_a \rightarrow -\infty$  and only keep  $\mathbf{F}$ , however, this does not change  $k_{\text{eff}}$  as  $\mathbf{F}$  is assumed to have a positive mass in the renormalization; see Tong's lectures [37] for a nice discussion. The effective CS levels are naturally selected by plumbing graphs, as we only consider integral surgeries, which have nice Kirby moves and handle slides (2.21). This geometric change caused by decoupling is analogous to the handle-slide that can be interpreted as twists, although the former contains different information and is not an equivalent transformation. After this inequivalent Dehn twist or decoupling, the framing number describing effective CS levels changes significantly  $\bullet_k \rightarrow \bullet_{k+q^2}$ . We will revisit this twist in the paragraph below (4.12).

### 3.4 3d theories from Lens spaces

In this subsection, we investigate the theories that can be engineered by Lens spaces. Firstly, it is free to add many defect M5-branes on Lens spaces  $L(k, 1)$ . These M5-branes can only be parallel to each other, as the longitude  $S_0^1$  is unique for Lens spaces. However, we can

<sup>9</sup>This indicates the 3d brane webs for charge  $q$  matters as well.

distinguish them by tuning on different mass parameters  $m_i$  and winding numbers  $q_i$ . Thus Lens spaces with Lagrangian defects can engineer a class of theories<sup>10</sup>:

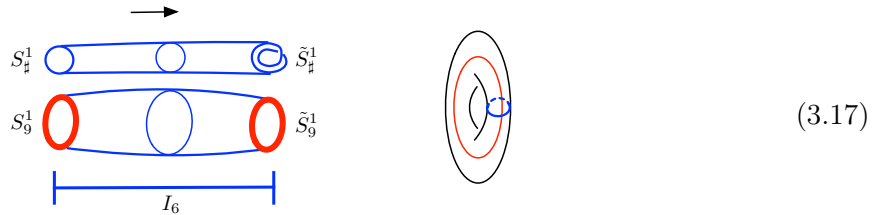
$$U(1)_k + \oplus_{i=1}^{N_f} \mathbf{F}_{q_i} + \oplus_{i=1}^{N_a} \mathbf{A}\mathbf{F}_{q'_i}, \quad (3.15)$$

where  $N_f$  is the number of defect M5-branes, and charge  $q_i$  are the winding numbers of Lagrangian M5-branes on the matter circle  $S^1_9$ . For instance, one can introduce two defects on the same solid torus:



It is obvious that when matter circles coincide, Lagrangian defects coincide as well and the flavor symmetry is enhanced to  $U(N_f)$ . This fusion of defects is interesting and complicated, and we would like to leave it for future work.

The matter circle and gauge circle can be easily identified, as they are longitude  $S^1_9$  and meridian  $S^1_{\sharp}$  of the torus  $T^2_{9\sharp}$  respectively. We use the following figure to illustrate the parallel transport of these two circles from one endpoint to the other:



If we cut the  $I_6$  in the middle, then the left part is a solid torus  $D^2 \times S^1_9$ , so the parallel transport (movement) of matter circles is the deformation of circles from the core to the bulk of the solid torus. The theory is totally determined by defects and the gluing map that fixes the framing numbers  $k$ .

The matter circle  $S^1_9$  can be viewed as the flavor D5. The circle  $S^1_{\sharp}$  associates to NS5 and can be called gauge circles, because NS5 can transport to the other endpoint and picks up an angle, and D3-brane in between lives the gauge groups. The correspondence between the solid torus and a sub-web is:



The gauging of D3-brane is described by gluing two solid tori, or adding a NS5 to the sub-web.

<sup>10</sup>Note that  $\mathbf{A}\mathbf{F}$  can be viewed as  $\mathbf{F}$  with the opposite charge.

## 4 Surgery circles and matter circles

In the last section, we analyzed Lens space  $L(k, 1)$ . However, a Lens space can only engineer theories with one gauge node  $U(1)_k$ , and hence are not generic. The generic three-manifolds are obtained by Dehn surgeries on links of circles (plumbing graphs). In this section, we will discuss how to introduce defect M5-branes that are consistent with Dehn surgeries, and see how they relate to geometric transformations.

### 4.1 Dehn surgeries and $ST$ -moves

Lens spaces are building blocks of any closed orientable three-manifolds, namely

$$M_3 = L(k_1, 1) \sqcup L(k_2, 1) \sqcup \cdots \sqcup L(k_n, 1), \quad (4.1)$$

for which the surgery circles for Lens spaces are linked to each other, and people often use the link  $L_1 \cup L_2 \cup \cdots \cup L_n$  to represent the  $M_3$ . Recall that plumbing graphs denote this link by the rules that  $L_i \rightarrow \bullet_{k_i}$  and  $L_i \cup L_j \rightarrow \bullet_{k_i} - \bullet_{k_j}$ . Explicitly, a closed  $M_3$  is obtained by drilling out the neighborhood of the link and gluing back many solid tori:

$$M_3 := S^3 \setminus (L_1 \cup L_2 \cup \cdots \cup L_n) := (S^3 - \cup_{i=1}^n N(L_i)) \sqcup_{f_i} (\oplus_{i=1}^n D_i^2 \times S^1). \quad (4.2)$$

which is the definition of Dehn surgery that is illustrated in Figure 1. The neighborhood of each surgery circle  $L_i$  is  $N(L_i) := D_i^2 \times L_i$ , and each solid torus is  $D_i^2 \times S^1$ . The gluing map  $f_i$  maps the boundary of the  $i$ -th solid torus to the boundary of the  $i$ -th link complement. Note that these solid tori  $D_i \times S^1$  are independent and hence there is no need to consider if they are linked before gluing in. Moreover, the knot complement  $S^3 - N(K)$  is called knot exterior, whose boundary is a torus even though the  $K$  is knotted.

The Dehn surgery provides more details on the gluing map  $f_i$ , which is determined by the meridian  $\alpha_i$  of the solid torus  $D_i^2 \times S^1$  and a curve  $J_i$  on the boundary of the complement  $S^3 - N(L_i)$ , namely  $f_i(\alpha_i) = J_i$ . Therefore, the gauge circle as the meridian  $\alpha_i$  is analogous to the circle  $L_i$ . Moreover, the Dehn surgery for Lens spaces differs from gluing two solid tori by the torus switch which is defined as exchanging meridian and longitude  $\alpha_i \leftrightarrow \beta_i$ . Therefore the gluing map (3.6) is transposed in the surgery description and the images of the meridian and longitude of solid torus  $D_i^2 \times S^1$  are

$$\begin{bmatrix} f_i(\alpha_i) \\ f_i(\beta_i) \end{bmatrix} = \begin{bmatrix} k_i & -1 \\ 1 & 0 \end{bmatrix} \cdot \begin{bmatrix} \alpha_i \\ \beta_i \end{bmatrix}, \quad (4.3)$$

where the gluing map  $f_i := f_{k_i}$  is represented as a matrix depending on its framing number  $k_i$ . The longitude  $\beta_i$  of the boundary of  $S^3 - N(L_i)$  represents the surgery circle  $L_i$ , and the Jordan curve is  $J_i = k_i \alpha_i - \beta_i$ , since this gives to the right framing number by the definition  $L_i \cdot L_i := \beta_i \cdot J_i = k_i$ .

**$ST$ -moves and matter circles.** In the last section, using M-theory/IIB duality we find matter nodes on plumbing graphs do indeed exist and should be the matter circles given by defect M5-branes, and the charge  $q$  of the matter is the winding number between gauge

circle and matter circle. Therefore, one can draw a link graph for the plumbing theory below:

$$(4.4)$$

Matter circle and gauge circle should form a Hopf link in each solid torus (3.18). In this note we use red and blue colors for link graphs to distinguish matter node and gauge node respectively. One can add many matter nodes on the same gauge node, then correspondingly many matter circles (red circle) should link to the gauge circles (blue circle). Changing the orientation of circles flips the signs of charges.

Note that at this stage the matter circle  $\bigcirc$  is just a circle given by the intersection of the Lagrangian defect with three-manifolds. Thus one cannot apply Dehn surgery on the matter circle. In section 4.4, we will show that matter circle relates to the three-sphere  $S^3_\infty$ , and there is naturally an identical surgery on the neighborhood of  $\bigcirc$ .

**Multiple charged matter.** In the above example, one can see that the matter circle can bring matters in the fundamental representation to plumbed manifolds. There could be matters charged under many gauge nodes, such as bifundamental chiral multiplets, trifundamental, and so on, depending on how many gauge circles are linked by the matter circle. Multi-charged matters can be obtained by  $ST_\beta$ -moves from the fundamental matters on the special Lens space  $\bullet_{\pm 1} - \blacksquare$  as shown in (2.22). In the link graph, one can also directly link the universal fundamental matter circle to many gauge circles to get a multi-charged matter. For example, a bifundamental matter is represented by

$$(4.5)$$

These two ways of introducing multi-charged matter are equivalent and are related by  $ST_\alpha$ -moves.

## 4.2 Images of matter and gauge circles

Both gauge circles and matter circles are useful to identify 3d theories. As we have reviewed in section 4.1, the images of meridians  $\alpha_i \mapsto J_i$  determine the three-manifolds. One may guess that the images of the longitude  $\beta_i$  determine matters. However, the answer is tricky as there are equivalent twists. In this section, we discuss Lens spaces to partly solve this problem. We find various properties of matter circles are highly consistent with 3d brane webs in section 3.2, which motivates us to find a geometric interpretation for  $ST$ -moves in section 4.4.

**Lens spaces  $L(k, 1)$ .** The Lens space is given by  $S^3 \setminus \bigcirc_k := S^3 - N(\bigcirc) \cup_{f_k} (D^2 \times S^1)$ . We denote the meridian and longitude of the solid torus as  $(\alpha, \beta) := ((S^1, *), (*, S^1)) \subset D^2 \times S^1$

where  $*$  denotes a point on  $D^2$  or  $S^1$ , and that of the complement  $S^3 - N(\bigcirc)$  as  $(\alpha', \beta')$ , which in other words are the meridian and longitude of the surgery circle.

The gluing map  $f$  is from the boundary of solid torus to the boundary of the complement. For convenience, we denote  $\text{Im}(\alpha) = f(\alpha)$  and  $\text{Im}(\beta) = f(\beta)$ , and then we have

$$\begin{bmatrix} f(\alpha) \\ f(\beta) \end{bmatrix} = \begin{bmatrix} p & -q \\ r & s \end{bmatrix} \cdot \begin{bmatrix} \alpha' \\ \beta' \end{bmatrix}, \quad (4.6)$$

where the determinant of the matrix should be one, namely  $ps + qr = 1$  (unitary condition) as the mapping class group is  $SL(2, \mathbb{Z})$ . In addition, the Jordan curve is  $J = \text{Im}(\alpha) = p\alpha' - q\beta'$  which is a torus knot  $T_{-q,p}$  on the boundary of the complement.

For a Lens space  $L(k, 1)$ , we have  $p = k$  and  $q = 1$ , so  $r = -sk + 1$  for any  $s \in \mathbb{Z}$  could satisfy the unitary condition, which gives infinite many equivalent gluing maps. The images of gauge and matter circle on the complement read

$$\begin{aligned} f(\alpha) &= k\alpha' - \beta', \\ f(\beta) &= (-sk + 1)\alpha' + s\beta' = \alpha' - s(k\alpha' - \beta') = \alpha' - sf(\alpha). \end{aligned} \quad (4.7)$$

Recall that the framing number is defined as the linking number between the image of meridian and the longitude of complement, namely  $f(\alpha) \cdot \beta' = k$ . One can see that the image of matter circle  $f(\beta) = \text{Im}(\beta)$  contains  $s$ -Dehn twists of the image  $f(\alpha)$ . We should set  $s = 0$  to fix this free integer, and then  $f(\beta) = \alpha'$  leads to a D5-brane. The matter D5-brane should be invariant under the transport as shown in Figure 4. Otherwise, D5-brane on one endpoint would become a charge  $(-sk + 1, s)$  5-brane on the other endpoint, which does not make much sense for 3d brane webs expect a special case.

In short,  $(f(\alpha), f(\beta)) = (k\alpha' - \beta', \alpha')$ . The image of matter circle  $\beta$  is fixed and is always the meridian  $\alpha'$  of the torus boundary of the complement. This is consistent with the circle graph in (4.4). The special case is that when  $s = \pm 1$  and  $k = \pm 1$ , the image of matter circle is  $f(\beta) = \pm\beta'$ . This means that a D5-brane transforms to a NS5-brane. This is the exceptional 3d brane web in (3.9), which also gives  $\bullet_{\pm 1} - \blacksquare$  after decoupling the **AF**. In this sense,  $L(\pm 1, 1)$  are quite special, as both  $\alpha'$  and  $\beta'$  can be matter circles.

The integer  $s$  can also be fixed from another perspective. Note that the linking number of gauge and matter images is  $f(\alpha) \cdot f(\beta) = 2sk - 1$ . It is natural to set  $s = 0$ , such that  $f(\alpha) \cdot f(\beta) = -1$ , which could ensure that matter circle has winding number  $\pm 1$  with gauge circle. Since the winding number is the charge of matter, it should be preserved under the deformation of the OV-defect. For  $L(\pm 1, 1)$ , we can also have  $f(\alpha) \cdot f(\beta) = 1$  if  $s = \pm 1$ .

**Three-sphere  $S^3$ .** For  $L(1, 0) = S^3_\infty$ , the meridian of solid torus  $\alpha$  maps to  $J = \alpha'$  on the boundary torus of  $S^3 - N(\bigcirc)$ , and the longitude  $\beta$  maps to  $r\alpha' + \beta'$ . In short,

$$(f(\alpha), f(\beta)) = (\alpha', r\alpha' + \beta'). \quad (4.8)$$

$L(1, 0)$  defines the identical (trivial) surgery along the circle  $\bigcirc_\infty$ , which is obtained by filling in the same solid torus that was drilled out, so  $(\alpha, \beta) \mapsto (\alpha', \beta')$ , which fixes  $r = 0$ . In addition, although it is an identical gluing, if taking into account the torus switch, we can

see an unusual replacement: NS5  $\rightarrow$  D5 and D5  $\rightarrow$  NS5. This also gives a  $U(1)_0 + 1\mathbf{F} + 1\mathbf{AF}$ , but the role of NS5 and D5 are flipped on two endpoints. We use the brane web below to illustrate:

(4.9)

Therefore, identical surgery also leads to the exceptional brane web, which describes the self-dual 3d  $\mathcal{N} = 4$   $T[U(1)]$  theory with a D5-brane as shown in (3.9).

**L(1, n).** Note that  $L(1, n)$  for any  $n \in \mathbb{Z}$  give the same three-sphere  $S^3$ . One can understand  $L(1, n)$  by thinking about how to equal it to  $L(1, 0)$ . This  $n$  is the number of Dehn twists that redefine the circles on the complement  $S^3 - N(\bigcirc)$  by  $\alpha' = \alpha'' + n\beta''$ ,  $\beta' = \beta''$ , which is an equivalent surgery and this twist is called Rolfsen's twist [38]. Taking this twist into (4.8), we get the images of gauge circle  $\alpha$  and matter circle  $\beta$  below:

$$\begin{aligned} f(\alpha) &= \alpha'' + n\beta'', \\ f(\beta) &= r\alpha'' + (rn + 1)\beta'' = r(\alpha'' + n\beta'') + \beta'' = rf(\alpha) + \beta'', \end{aligned} \tag{4.10}$$

where  $(\alpha'', \beta'')$  are meridian and longitude on the boundary of the complement of  $L(1, n)$  after twist. Once again, the image of matter circle contains  $r$  copies of the image of meridian. Just like Lens space  $L(k, 1)$ , we can use the linking number constraint  $f(\alpha) \cdot f(\beta) = 2nr + 1 = \pm 1$  to find some special  $r$  and  $n$ . It is better to set  $r = 0$ , such that we always have  $f(\beta) = \beta''$  for any  $n$ . If we set  $nr = -1$  and then  $f(\beta) = r\alpha''$ , which means the image of matter circle  $\beta$  is the meridian  $\alpha''$  of the surgery circle, and in particular  $r = \pm 1$  is more meaningful for the presence of matter nodes. Once again, this property coincides with the special case of brane web that we discussed in section 3.2.

Another way to understand this  $r$ -integer is the Dehn twists of  $\beta'$  along  $\alpha'$ , namely  $\beta' = \beta'' + t\alpha''$ ,  $\alpha' = \alpha''$ , which could cancel this freedom  $r$ -integer in (4.8) by setting  $t = -r$ , and then this returns  $L(1, 0)$ . This can be interpreted as the  $SL(2, \mathbb{Z})$  transformation for brane webs. The brane web for  $L(1, n)$  can be transformed into brane webs in (3.9), where the matter circle D5 on one endpoint of D3-brane is mapped also to a NS5 on the other endpoint of D3. If  $n = \pm 1$ ,  $r = \mp 1$ , then  $f(\alpha) = \mp \alpha''$ . Once again, one can see  $L(1, \pm 1)$  are special. As the NS5-brane in this case can be transformed to a D5, which is shown in the first web in (3.8). Here, we use the deformation of torus to illustrate this special twist:

(4.11)

The red line as the matter circle maps to either longitude or meridian when  $k = \pm 1$ , and these two cases are S-dual to each other and should be equivalent. When one chiral multiplet is decoupled properly, they both lead to the same brane webs for  $\bullet_{+1} - \blacksquare$ .

An observation is that (4.7) and (4.10) are equivalent if meridian and longitude are exchanged, however the properties of  $L(k, 1)$  and  $L(1, n)$  are significantly different, so one cannot switch meridian and longitude randomly.

$\mathbf{S}^2 \times \mathbf{S}^1$ . This geometry  $\bullet_0$  is very useful for the connected sum of three-manifolds, such as  $\bullet_{k_1} - \bullet_0 - \bullet_{k_2} = \bullet_{k_1+k_2}$ . For  $L(0, 1) = S^1 \times S^2$ , the images of meridian and longitude are

$$(f(\alpha), f(\beta)) = (-\beta', \alpha' + s\beta'). \quad (4.12)$$

We have to set  $s = 0$  to preserve the charge of D5-brane. If we perform the Dehn twist  $\alpha' = \alpha'' + t\beta''$  and  $\beta' = \beta''$ , then the  $s$ -twist can be canceled by setting  $t + s = 0$ . If we perform the twist  $\alpha' = \alpha''$  and  $\beta' = \beta'' + m\alpha''$ , then we get  $f(\alpha) = m\alpha'' - \beta''$ ,  $f(\beta) = (-sm + 1)\alpha'' + s\beta''$ . This turns  $L(0, 1)$  into a Lens space  $L(m, 1)$ , so the Dehn twist of  $\beta''$  is not an equivalent operation, but a geometric transition that describes the decoupling of matters. Hence  $L(0, 1)$  is very sensitive to the Dehn twist along meridian. This property is consistent with the decoupling of  $\mathbf{AF}$  as shown in (3.14), which tells the twist  $\beta' = \beta'' + m\alpha''$  namely  $S_{\sharp}^1 \rightarrow S_{\sharp}^1 + mS_9^1$  changes geometry. Therefore, one can view the decoupling of the matter  $\mathbf{AF}$  with a charge  $m$  as this particular Dehn twist. This reminds us that twists have different types and play different roles in different contexts. Some of them lead to equivalent surgeries, but others changes the geometry.

$\mathbf{L}(\pm 1, 1)$ . From the above analysis, one can see that  $L(\pm 1, 1)$  are special cases, whose images of matter circles can be on either meridian or longitude of the complement, depending on equivalent Dehn twists one prefers. If one views  $L(\pm 1, 1)$  as the three-sphere, the image of matter circle is on longitude  $\beta'$ , and if as standard Lens spaces, then the matter image is on meridian  $\alpha'$ . These two locations should be equivalent, which motivate us to interpret this as mirror duality. To prove that, there are still a few steps and we leave it to next section. We summarize the images of matter circles in Table 3<sup>11</sup>.

	$L(k, 1)$	$L(1, n)$	$L(\pm 1, 1)$	$L(1, 0)$	$L(0, 1)$
Im( $\alpha$ ) of gauge circle $\alpha$	$k\alpha' - \beta'$	$\alpha' + n\beta'$	$\alpha' \pm \beta'$	$\alpha'$	$-\beta'$
Im( $\beta$ ) of matter circle $\beta$	$\alpha'$	$\beta'$	$\alpha' \xleftrightarrow{\text{twist}} \beta'$	$\beta'$	$\alpha'$

**Table 3.** In this table, we summarize the possible locations of gauge circles and matter circles for various Lens spaces.

### 4.3 Matter circles and cobordism

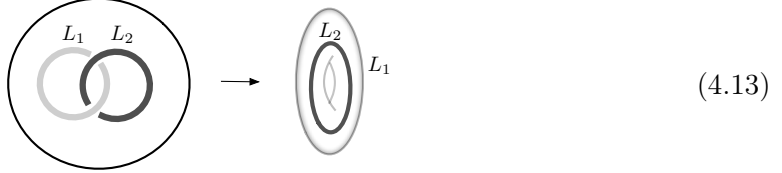
There are many linked gauge circles in a generic three-manifold, and hence many possible locations for matter circles. In this section, we discuss three-manifolds beyond Lens spaces, using cobordism.

**Hopf link cobordism.** One basic example is the Hopf link complement. To obtain it one should drill out two solid tori. After drilling out the first solid torus  $N(\bigcirc)$ , one gets a complement which is also a solid torus if taking the interior of its torus boundary to the outside, namely  $S^3 - N(\bigcirc) = D^2 \times S^1$ . In this process, the meridian and longitude are exchanged, which is a torus switch. One can denote it by  $S^3 - N(\bigcirc) := \tilde{N}(\bigcirc)$ . Before

<sup>11</sup>If one translates surgery into the description of gluing two solid tori, then the torus switch  $\alpha' \leftrightarrow \beta'$  should be applied.

drilling out the second solid torus, recall that in the complement of Hopf link, the meridian  $\alpha_1$  (longitude  $\beta_1$ ) of the first  $N(\mathbb{O}_1)$  could deform to the longitude  $\beta_2$  (meridian  $\alpha_2$ ) of the second  $N(\mathbb{O}_2)$ . Therefore, if we take the inside of torus boundary to outside, the meridian  $\tilde{\alpha}_1$  of  $\tilde{N}(\mathbb{O}_1)$  will deform to the  $\alpha_2$ , and similarly  $\tilde{\beta}_1$  to  $\beta_2$ .

This geometry can be viewed as a solid torus with a torus hole inside. We illustrate Hopf link complement  $S^3 - N(\mathbb{O}_1 \# \mathbb{O}_2) = \tilde{N}(\mathbb{O}_1) - N(\mathbb{O}_2)$  as follows

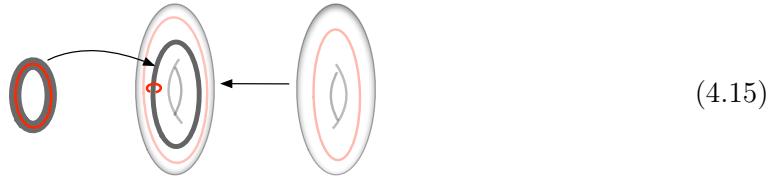


from which it is obvious to see how the surgery circles of  $N(L_1)$  and  $N(L_2)$  are related. The topology of this cobordism is a torus bundle  $T^2 \hookrightarrow M_3 \rightarrow I$ . One can slice it into foliations and each slice is a torus. We use the figure below to illustrate



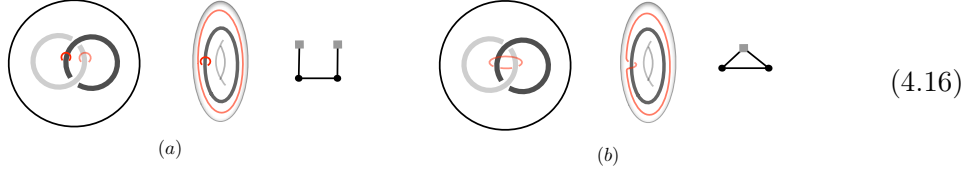
where the bulk is the inside of solid torus given by  $L_1$ , and on left and right endpoints of the interval  $I$  locate the torus boundaries of  $L_1$  and  $L_2$  respectively. The matter circle of  $L_1$  is the longitude, which can be freely moved in the bulk, while that of  $L_2$  is the meridian, as shown in the figure in (4.14). Note that in this cobordism, longitude (meridian) on the left boundary parallelly transports to longitude (meridian) on the right boundary, although roles played by these circles are switched on two boundaries.

To get the closed three-manifold given by surgery along the Hopf link, one can fill in a solid torus to the boundary of  $L_2$  and glue another solid torus to the boundary of  $L_1$ :



In this process, one can introduce matter circles, whose images are shown in the above graph. Notice that filling in a solid torus for  $\mathbb{O}_2$  is a surgery, while gluing back the solid torus for  $\mathbb{O}_1$  leads to a Lens space. The matter circles introduced by this surgery are not linked, but generically, two matter circles have diverse ways to tangle or fuse with each other, which may involves non-trivial phenomenon and we prefer to solve it in future. We

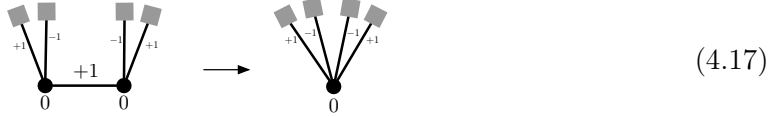
show two more examples below to illustrate other matter circles:



Note that in the graphs in (4.16), although we only draw the Hopf link complement, we assume solid tori have been glued back.

Moreover, for generic Hopf links with the linking number  $\mathcal{O}_1 \cdot \mathcal{O}_2 = k_{12} > 1$ , one can still take the boundary of  $N(\mathcal{O}_1)$  to the outside to get the a solid torus  $\tilde{N}(\mathcal{O}_1)$ , but the  $N(\mathcal{O}_2)$  would wind  $k_{12}$  times.

It is easy to read off the theories determined by this torus cobordism. Let us first investigate the three-manifold in (4.15), which is a three-manifold with two matter circles:  $M_3(\mathcal{O}_1, \mathcal{O}_2) = (S^3 - N(\mathcal{O}_1 \cup \mathcal{O}_2)) \sqcup (D^2 \times S^1) \sqcup (D^2 \times S^1)$ . The theory for a solid torus with a defect is a hypermultiplet, namely  $T[D^2 \times S^1] = \mathbf{1F} + \mathbf{1AF}$ , which reduces to a chiral multiple if the  $\mathbf{AF}$  is decoupled. In addition, Hopf link carries a mixed CS level  $k_{12} = +1$ , which encodes  $T[U(1)]$  theory [36]. Therefore, we get a gauged  $T[U(1)]$  theory with two D5-branes. If the framing numbers are zero, the theory is described by the plumbing graph below:



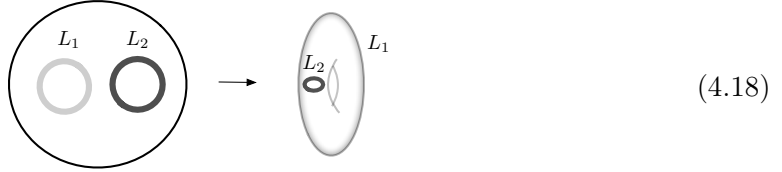
where we perform a S-duality on the hypermultiplet to get the right graph [1], which represents the theory  $U(1)_0 + 2\mathbf{F} + 2\mathbf{AF}$ , and this theory is exactly the self-dual  $T[SU(2)]$  theory in [36]. The above analysis lightly indicates the argument that the Hopf link complement could engineer some self-dual  $T[SU(N)]$  theories.

In [39], Demofte and Gaiotto found similar geometries from a different perspective. We think the construction in this note has some gaps to match with their constructions, since there-manifolds that we use have no boundaries, while these from gluing tetrahedrons often have singular torus boundaries (which are called torus cusps) since the tips of tetrahedrons are truncated; see also [14].

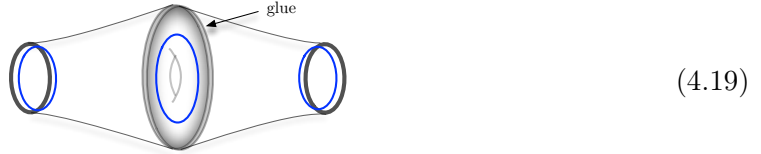
The operation of gluing back a solid torus with an OV-defect to the complement  $M_3 - N(L_i)$  can be interpreted as gauging global symmetries, and each OV-defect is associated with a global symmetry. However, if defects are not introduced, there is no flavor symmetry and no matter. We expect the global symmetry carried by torus boundaries of complement to be topological symmetries, as it matches the argument that after gauging the global symmetry becomes gauge symmetry. Through gauging, framing numbers as Chern-Simons levels can be introduced.

**Gluing cobordisms.** If  $\mathcal{O}_1$  and  $\mathcal{O}_2$  are not linked, then we have the complement  $S^3 - N(\mathcal{O}_1 \cup \mathcal{O}_2) = T^2 \times I$ , which can be obtained by truncating two poles of the two-sphere in  $S^2 \times S^1$ . This geometry is a trivial bundle with  $S^1$  fibered over a tube, and hence

could be used to connect two three-manifolds. For instance, the connected sum of two Lens spaces  $L(k_1, 1) \# L(k_2, 1)$  can be obtained by surgeries along  $L_1$  and  $L_2$ . Let us represent its complement below:



To get the a similar description using cobordisms, we can glue two Hopf link complements in (4.14):



where circles could transport in the bulk freely. The evolution of meridian and longitude from left to right is  $\alpha \mapsto \alpha \mapsto \alpha$  and  $\beta \mapsto \beta \mapsto \beta$ . This looks like a mirror reflection at the middle of the interval.

If gluing two Hopf link complements  $L_1 \cup L'_2$  and  $L_2 \cup L_3$  by identifying  $L'_2$  and  $L_2$ , one could get a more generic Hopf link  $L_1 \cup L_2 \cup L_3$ , whose cobordism is



where the torus switch needs to be applied to glue the exterior torus of  $L'_2$  and to the interior torus of  $L_2$ . The transformations of circles are  $\alpha \mapsto \alpha \xrightarrow{\text{switch}} \beta \mapsto \beta$  and  $\beta \mapsto \beta \xrightarrow{\text{switch}} \alpha \mapsto \alpha$ .

Moreover, the cobordism in (4.20) can be further extended to complicated links, such as the triangle in (2.22). We expect any closed oriented three-manifolds expressed by plumbing graphs can be represented by cobordisms. This looks like JSJ (Jaco-Shalen, Johannson) decomposition in geometric topology, which says many three manifolds can be decomposed along incompressible tori.

**Seifert manifolds.** Note that the cobordism in (4.19) is almost a Seifert three-manifold. The Seifert manifolds are given by Dehn surgeries on the torus boundaries of particular circle bundles over Riemann surfaces, namely  $M_3^{\text{Seifert}} := (S^1 \times \Sigma_{g,n}) \sqcup_{f_i} (D^2 \times S^1)_i$  where the  $S^1$  is fibered over the Riemann surface with genus  $g$  and  $n$  punctures. Then this bundle has  $n$  boundary tori (cusps), on which solid tori can be filled in through gluing maps  $f_i$ . When  $g = 1$  and  $n = 1$ , the geometry is  $S^1 \times S^2 \setminus N(\bigcirc_i)$ , while the cobordism in (4.19)

is  $S^3 \setminus N(\bigcirc_i)$ , so they differ a little, which should however be equaled by slightly changing gluing maps. When  $g > 0$ ,  $S^1 \times \Sigma_{g,n}$  can be cut into  $2g$  numbers of building blocks  $S^1 \times S^2 \setminus \{\circ_1, \circ_2, \dots\}$  with two or three punctures. The meridians of boundary tori are associated to punctures  $\circ_i$ , and the longitudes to the  $S^1$ ; see e.g. [40] for more details on Seifert manifolds. There could be diverse ways to put matter circles on Seifert manifolds, which we think is an open problem.

#### 4.4 $ST$ -moves as Rolfsen's surgery twist

The 3d-3d correspondence tells that the 3d complex Chern-Simons theory on  $M_3$  corresponds to the 3d  $\mathcal{N} = 2$  theory  $T[M_3]$  determined by the three-manifold  $M_3$ . The surgery construction of 3d theories in our context is in complement with the DGG/GPV construction. When the matter fields are introduced by defect M5-branes, the corresponding objects on 3d CS theory relate to Wilson loops. For other works on the defect extensions of 3d-3d correspondence, see [41].

**Witten's surgery treatment.** We borrow an inspiring idea from Witten's work [42]: the 3d CS theory on  $S^3$  with the Wilson loop along the knot  $K$  can be equivalently described by the CS theory on  $M_3 = S^3 \setminus K$ , which is obtained by a Dehn surgery along  $K$ . This work shows that knot can be studied on its neighborhood which is a solid torus  $K \times D^2$ .

This equivalent treatment reminds that one can not only freely connects a three-sphere to a three-manifold  $S^3 \# M_3 = M_3$ , but also freely glue a  $S_\infty^3$  to a three-manifold, and this however does change the manifold, namely  $M_3 = M_3 \sqcup S_\infty^3$ . The  $S_\infty^3$  is  $L(1,0)$  which is obtained by the identical surgery along a circle  $\bigcirc_\infty$ . Recall that the identical surgery is the process of cutting out a solid torus along a circle and then fill in the same solid torus, so the three-manifold does not change. Note that this circle is the longitude of the complement and can freely link to the  $K$  that determines  $M_3$  even if in a complicated pattern, so we use the symbol  $\sqcup$  rather than the symbol for connected sum  $\#$ .

In the presence of the matter circle  $\bigcirc$  in a three-manifold  $M_3$ , one can still perform an identical surgery along the neighborhood of  $\bigcirc$ , such that the  $\bigcirc$  is given a framing number  $\bigcirc_\infty$ . In this sense, on the neighborhood of the matter circle, naturally there is an identical surgery. The matter circle  $\bigcirc_\infty$  is hence a typical example that Witten's equivalent treatment applies. One can either firstly introduce a matter circle  $\bigcirc$  and then perform identical surgery, or reverse the process. These two processes are commutative, and hence we have

$$M_3 \setminus \bigcirc_\infty = M_3 \sqcup (S_\infty^3 \setminus \bigcirc). \quad (4.21)$$

Since  $S_\infty^3$  has an infinite framing number, it is not very confusing if directly interpreting it as the CS level, as an infinite CS coupling gives vanishing contribution in the Lagrangian description. But still it is confusing to treat  $\infty$  by surgery. Fortunately, one can use the Rolfsen's rational equivalent surgery calculus in [38] to equivalently transform it into  $L(\pm 1, 1) \setminus \bigcirc$ .

**Rolfsen's twist and rational equivalent surgeries.** The Rolfsen's twist leads to a rational equivalent surgery that changes linking numbers of circles, which is basically a

Dehn twist on meridian by  $\text{Im}(\alpha) = \alpha' + t\beta'$  that we have shown in (4.10), and this twist turns  $L(1,0)$  into  $L(1,t)$ . If we perform  $t$  numbers of Rolfsen's twists on a circle  $L$ , then it also twists circles  $L_i$  that link to  $L$ . Suppose the surgery circle sets  $\{L\}$  have linking numbers as follows

$$L_i \cdot L_i := k_i, \quad L_i \cdot L_j := k_{ij}. \quad (4.22)$$

After the twist on  $L$ , the new circle  $\tilde{L}$  has a linking number as follows

$$\tilde{L} \cdot \tilde{L} = \tilde{k} = \frac{1}{t + \frac{1}{k}}, \quad t \in \mathbb{Z}. \quad (4.23)$$

If  $L_i$  and  $L_j$  do not link to  $L$ , then  $\tilde{L}_i \cdot \tilde{L}_j = L_i \cdot L_j = k_{ij}$ . If either  $L_i$  or  $L_j$  links to  $L$ , then  $\tilde{L}_i \cdot \tilde{L} = L_i \cdot L$ . If either  $L_i$  or  $L_j$  link to  $L$ , then

$$\tilde{L}_i \cdot \tilde{L}_j = L_i \cdot L_j + t(L_i \cdot L)(L_j \cdot L), \quad (4.24)$$

which is similar to Kirby move of first type. It is more convenient to use a graph to illustrate:

$$\begin{array}{ccc} \begin{array}{c} \bullet k_i \\ \diagup \quad \diagdown \\ a \quad \quad b \\ \bullet k \quad \bullet k_j \\ \diagdown \quad \diagup \\ b \quad \quad a \\ \bullet k_j \end{array} & \xrightarrow{\text{Rolfsen's twist}} & \begin{array}{c} \bullet k_i + t a^2 \\ \diagup \quad \diagdown \\ a \quad \quad b \\ \bullet \frac{1}{t + \frac{1}{k}} \quad \bullet k_j + t b^2 \\ \diagdown \quad \diagup \\ b \quad \quad a \\ \bullet k_j + t b^2 \end{array} \end{array} \quad (4.25)$$

This equivalent surgeries put strong constraints on framing numbers, since the later should be integral numbers. This type of equivalent surgeries does not fall in the class of Kirby moves, and is called rational calculus found by Rolfsen in [38].

**Geometric interpretation for  $ST$ -moves.** We now show that Rolfsen's twist can be interpreted as  $ST_\alpha$ -moves. Firstly, we perform a drilling chain trick in Figure 6. The map (a) is an artificial identical surgery on the matter circle  $\bigcirc$ . In map (b), the surgery is replaced by an equivalent rational surgery by a Rolfsen twist, which turns  $L(1,0) \setminus \bigcirc$  into  $L(\pm 1, 1) \setminus \bigcirc$ . Meanwhile, the positions of matter circles  $\bigcirc$  should be switched from longitude to meridian, as is shown in Table 3. In (c), one can continue the drilling and identical surgery along  $\bigcirc$ , and if using bare CS levels, the last graph will only differ to the second graph by a  $\bigcirc_{\pm 1}$  which can be integrated out by  $\alpha$ -Kirby moves, and hence the second and fourth graph only differ by the orientation. One can observe that the loop of maps (b)  $\rightarrow$  (c)  $\rightarrow$  (d) is the mirror triality ( $ST$ -moves). This gives to two types of  $ST$ -moves shown in (2.4).

If introducing a charge- $q$  matter on  $L(k,1)$ , we expect Rolfsen's twist with  $t = \pm 1$  could produce the linking graphs for  $ST_\alpha$ -move:

$$\begin{array}{ccc} \begin{array}{c} \bigcirc_{\infty} \\ \diagup \quad \diagdown \\ \bigcirc_k \end{array} & \longleftrightarrow & \begin{array}{c} \bigcirc_{\pm 1} \\ \diagup \quad \diagdown \\ \bigcirc_{k \pm q^2} \end{array} \end{array} \quad (4.26)$$

where we have assigned effective framing numbers. Following the twist rule, the charge  $q$  as the linking number is not changed. Note that after the Rolfsen's twist, the matter circle

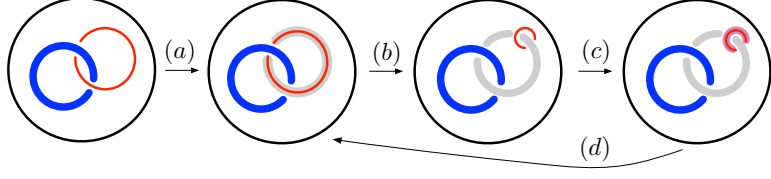


**Figure 6.** Using the drilling trick, identical surgery, and Rolfsen’s rational equivalent surgery, one can geometrically derive the  $ST_\alpha$ -move coming from physical analysis.

should not link to the previous gauge circle (blue circle). Moreover, since  $k$  is the effective CS level, we should assume it has already received quantum corrections from matters. A special case is  $S_\infty^3$ , since it has a  $\infty$ -framing number, any corrections from matters is absorbed into  $\infty$ . One can notice the linking numbers of circles in (4.26) match with that of  $ST$ -moves:

$$\begin{array}{c} \blacksquare \\ | \\ \bullet \\ k \end{array} \xrightarrow{ST} \begin{array}{c} \blacksquare \\ | \\ \bullet \\ k \pm q^2 \end{array} \begin{array}{c} \blacksquare \\ | \\ \bullet \\ \pm 1 \end{array} \quad (4.27)$$

which is equivalent to the graph in (2.4) and here we only assigned effective CS levels.

If ungauging the gauge group by deleting nodes  $\bullet_k$  and  $\bullet_{k+q^2}$ , the  $ST$ -move reduces to the basic mirror duality between  $1\mathbf{F} \leftrightarrow U(1)_{\pm 1} + 1\mathbf{F}$ :

$$\blacksquare \xleftrightarrow{\text{mirror}} \begin{array}{c} \blacksquare \\ | \\ \bullet \\ \pm 1 \end{array} \quad (4.28)$$

Correspondingly, ungauging is the operation of deleting the surgery circles in (4.26), which lefts with a  $L(1,0)$  with a matter circle  $\bigcirc$  on its longitude, and correspondingly a  $\bigcirc$  on the meridian of  $L(\pm 1, 1)$ . This mirror tuality can be represented as linking graphs:

$$\begin{array}{c} \bigcirc \\ \infty \end{array} \xleftrightarrow{\text{mirror}} \begin{array}{c} \bigcirc \\ \pm 1 \end{array} \quad (4.29)$$

This mirror duality is highly non-trivial, as it means that even if the matter circle (Lagrangian defect) is present, the rational twist is still a homomorphism, so the Rolfsen’s twist can be extend to the case with OV defect  $\bigcirc_\infty$  rather than only  $\bigcirc_\infty$ . Note that adding  $\bigcirc$  along the longitude of  $L(\pm 1, 1)$  is not allowed, because  $L(\pm 1, 1)$  should be viewed as a standard Lens space, on which the image of matter circle  $\bigcirc$  should be the meridian of the complement, as is shown in section 4.2. From the perspective of brane webs, the geometric interpretation in (4.29) is a local S-duality that switches NS5 and D5.

**FI and mass parameter revisited.** We draw the matter circle (red) big on the left graph and small on the right graph of (4.29), because the mirror map exchanges the FI parameter  $\xi$  of the gauge circle  $U(1)_k$  and the mass parameter  $m$  of the matter. One can conjecture that the length of the surgery circle represents the FI parameter, and the length of matter circles represents the mass parameter. This is confirmed by sphere partition

function computations for the mirror duality in [1] that the matter in the dual theory  $\bullet_{\pm 1} - \blacksquare$  is almost massless up to a quantum shift  $q^* = e^{i*\epsilon}$ , and the mass parameter of  $\blacksquare$  becomes the FI parameter in the dual theory  $\bullet_{+1} - \blacksquare$ . Therefore, in the right graph of (4.29), we draw a very small red circle to denote the matter circle  $\circ$ .

In section 3.1, we tried to use M/IIB duality to identify the corresponding geometric objects on 3-manifolds for FI and mass parameters, but were not very successful. However, using the geometric representation of the mirror duality, one can solve this tricky problem. In short, the length of surgery circle  $\circ$  should be the FI parameter, and the length of matter circle  $\circ$  should be the mass parameter. These circles correspond to  $S_{\mathbb{H}}^1$  and  $S_9^1$  respectively in the elliptic torus  $T_{9\mathbb{H}}^2$  of M-theory.

**A knot example.** Because of the  $ST$ -move, one can replace any unknotted matter circle by a gauge circle with a matter circle  $\circ \leftrightarrow \circ$ , even if the matter circle  $\circ$  is linked to knotted gauge circles.

Lickorish-Wallace theorem tells that any closed orientable three-manifold can be obtained by Dehn surgeries along a link in  $S^3$ , and each component of this link can be an unknot  $\circ$ . This means that if a three-manifold is given by surgeries along a knot  $M_3 = S^3 \setminus K$ , then this knot can be equivalently transformed into a class of links using Kirby moves. If a matter circle  $\circ$  is linked to a surgery knot  $K$ , one can still apply  $ST$ -moves. Here we illustrate a trefoil example in Figure 7.

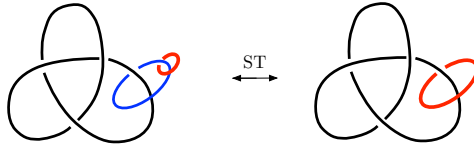
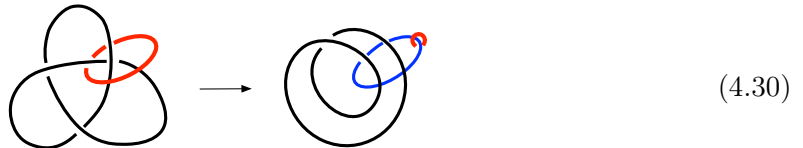


**Figure 7.** This three-manifold  $S^3 \setminus T_{2,3}$  is given by a Dehn surgery along a trefoil in  $S^3$ . The winding number between the blue circle  $\circ$  and trefoil  $K$  is the charge  $q$  for the matter. Here we insert a matter circle in a simple pattern.

One can consider complicated winding patterns between matter circles and knots. As a typical example in textbook e.g. [38, 40, 43], the trefoil can be unknotted by  $\alpha$ -Kirby moves into the link  $\bullet_k - \bullet_{\pm 1} - \blacksquare$  with linking number  $\pm 2$ . We can also do this by moving the matter circles  $\circ_{\infty}$  by  $ST$ -moves:



where a charge-2 matter circle is on the left graph, which after a  $ST$ -move generates a blue circle  $\bullet_{\pm 1}$ .

Note that matter circles could tangle with trefoils in very complicated patterns, depending on how to insert matter circles. Essentially, the matter circle can be any element in the fundamental group of the knot complement  $\pi_1(S^3 - N(K))$ .

The rational equivalent surgery can reproduce similar linking graphs given by handle-slides in section 2. We know that it is freely to introduce a  $S_\infty^3$  but not  $S_\infty^3 \setminus \bigcirc$ . Fortunately, handle-slides, such as (2.22) could tell how to introduce it. We firstly need to introduce  $S_{\pm 1}^3 \setminus \bigcirc$  and then apply the handle-slide operation by recombining gauge circles. Finally, we apply Rolfsen's rational twist to get  $S_\infty^3 \setminus \bigcirc$ . We use the following graph to illustrate this process:

$$\begin{array}{c}
 \text{grey circle } \pm 1 \quad \text{blue circle } k \quad \xrightarrow{K_\beta} \quad \text{linked circles} \quad \xrightarrow{\text{twist}} \quad \text{red circle } \infty \quad \text{blue circle } k \\
 \end{array} \tag{4.31}$$

where the twist is the reverse process of (b) in Figure 6. Bifundamental matter can also be introduced this ways as in (2.22).

For the linked matter circles, ST-moves may not be able to separate them, and computation shows linked matter circles are highly non-trivial. For instance,

$$\begin{array}{c}
 \text{two red circles} \neq \text{blue circle with two red circles} \quad \text{square with } n \neq \text{square with } n \text{ and } +1 \neq \text{square with } n \text{ and } 1+n^2 \\
 \end{array} \tag{4.32}$$

In addition, if a gauge circle  $\bullet_k$  links to a  $\bullet_\infty$ , we cannot directly apply Kirby moves of first type to integrate out  $\bullet_k$  to allow  $\bullet_\infty$  absorbs this node. Namely,  $\bullet_k = \bullet_k - \bullet_\infty \neq \bullet_\infty$ .

## 5 Open problems

The surgery construction discussed in this note depend only on the topology of three-manifolds, and translate dualities in terms of geometric structures. There are many open problems:

- One problem is to find the corresponding geometric structures for superpotentials. A basic cubic superpotential appears in SQED-XYZ duality. This duality encodes the cubic superpotential  $\mathcal{W} = XYZ$ , which is known to be a 2-3 move on hyperbolic geometry [14], but is not obvious through surgery. This basic duality has a gauged version, in which the superpotential is realized as relations between linking numbers of some triangle graphs [1]. We will provide the geometric interpretation for superpotentials in the coming work.
- One can expect a surgery construction for non-abelian theories. There could be some hints from Lens spaces. Once again, superpotentials should be carefully considered.
- The matter circles in this note are unknotted. Generically, matter circles could be knotted, which is known to be the Ooguri-Vafa construction of Jone polynomials. In this case, the OV defect intersects the three-manifolds along a knot  $K$ , namely  $L_K \cap M_3 = K$ , and the  $K$  is a knotted matter circle. If this matter knot  $K$  can be transformed into links of unknotted matter circles  $\bigcirc$ , the encoded gauge theories for knots can be read off, and more stories on knots can be told. One can possibly use

some topological invariants such as the RT-invariants of  $M_3 \setminus K$  to analyze the knotted matter circle  $K$ ; see e.g. [46].

- We expect the surgery construction could be a starting point to geometrically understand the knots-quivers correspondence [44, 45], and to add more details on the 3d-3d correspondence.
- There are multiple ways to put matter circles in three-manifolds, which can also be deformed and merged. This is similar to what happens in modular tensor category (MTC). The mapping class group of torus is useful to analyze the images of matter circles, but we have not fully solved this problem in this note.
- It is mysterious to match surgery constructions and conifold/large-N transitions of Lens spaces [47, 48]. It seems that there should be a fiber and base duality to connect these two concepts. It is because that in the large-N transition, the bulk Lens space corresponds to the flavor symmetry and the Lagrangian brane  $L_K$  corresponds to the gauge group, which is opposite to surgery construction.
- In [16, 39], a branched cover realization of 3d theories through 4d Seiberg-Witten curves is established, which is similar to our surgery construction in many aspects. We hope to find the relations between them in future.

## Acknowledgments

I would like to thank Satoshi Nawata for many useful discussions on Ooguri-Vafa construction for engineering matter, particularly when I was jumping between right and wrong. I am also grateful to Sung-Soo Kim, Jihua Tian, Yi-Nan Wang, and Fengjun Xu for helpful discussions, and the hospitality of UESTC, CHEP, and BIMSA where parts of this work was done. The work of S.C. is supported by NSFC Grant No.11850410428 and NSFC Grant No.12305078.

## A Some basics

### A.1 Lens space

Lens spaces are defined as the orbifolds of the three-sphere:  $L(k, 1) = S^3/\mathbb{Z}_k$ . if using complex coordinates, the three-sphere is  $|z_1|^2 + |z_2|^2 = r^2$ , and the orbifold  $\mathbb{Z}_k$  action is  $(z_1, z_2) \mapsto (e^{\frac{2\pi i}{k}} z_1, e^{\frac{2\pi i}{k}} z_2)$ . The homology of this geometry is  $H_1(L(k, 1)) = \mathbb{Z}_k$ . Some Lens spaces are typical geometries, such as  $L(2, 1) = S^3/\mathbb{Z}_2 = \mathbb{RP}^3$ . Lens spaces have many equivalences that  $L(p, q) = L(p, q + np) = L(-p, q)$ , so  $L(k, 1) = L(\frac{k}{nk+1}, 1)$ . The cotangent bundle of Lens spaces are Calabi-Yau three-manifolds. The Lens space as the base of  $T^*L(k, 1)$  is also a special Lagrangian submanifold. As special examples of Seifert manifolds, Lens spaces are circle fibered bundles over a two-sphere:  $\mathcal{O}(-k) \hookrightarrow L(k, 1) \xrightarrow{\pi} \mathbb{P}^1$ .

The plumbing manifolds are given by gluing a couple of Lens spaces. Each Lens space is obtained by performing a surgery along a circle with a framing number, namely  $L(k, 1) :=$

$S^3 \setminus \mathbb{O}_k = (S^3 - N(\mathbb{O})) \cup_k (D^2 \times S^1)$ . The Lens space is denoted by this surgery circle which is the longitude of the torus boundary of the complement  $S^3 - N(\mathbb{O})$ . The plumbing graph is a shorthand for the links of surgeries. For instance, the Lens space and Hopf link can be denoted:

$$\text{Diagram (A.1): } \begin{array}{ccc} \text{Circle } k & \longrightarrow & \bullet_k \\ \text{Linked circles } k_1, k_2 & \longrightarrow & \bullet_{k_1} \text{---} \overset{\pm 2}{\text{---}} \bullet_{k_2} \end{array}$$

where each black node denotes a Lens space  $L(k, 1)$ , and the linking numbers are assigned on the line connecting black nodes. Depending on orientations, linking numbers can be given different signs. By extending this example, complicated plumbing graphs that contain many nodes and lines denote generic compact three-manifolds given by Dehn surgeries.

The framing number is known to be the linking number between the surgery circle  $L$  and its slightly deformed circle  $L'$ . After deformation, these two circles have linking number  $L_i \cdot L_i := L_i \cdot L'_i = k_i$ . The linking number is a half of the crossing number between two circles:  $L_i \cdot L_j = k_{ij} := \frac{1}{2} \times \text{crossing number}$ . We only focus on integral surgeries, as the parity anomaly requires framing numbers to be integers [3].

## A.2 Lagrangian submanifolds

The geometry of Lagrangian manifolds is  $S^1 \times \mathbb{R}^2$  where  $\mathbb{R}^2 \subset \mathbb{R}^3$  which is a section in the fiber of the cotangent bundle  $T^*M_3$ . The intersection  $S^1 = (S^1 \times \mathbb{R}^2) \cap M_3$  is the matter circle. Topologically, the Lagrangian submanifold can be written as a solid torus  $S^1 \times D^2 = T^2 \times \mathbb{R}_+$  where the  $T^2$  degenerates to the matter circle  $S^1$  at the origin of  $\mathbb{R}_+$ . Hence, the Lagrangian submanifold is a half of  $S^1 \times S^2$  and locally admits a toric geometry description. We illustrate a more precise description of the Lagrangian submanifold of Ooguri-Vafa type as follows



where the  $L_K$  does not really intersect the Lens space, but these two are connected by a M2-brane which is a tube that can be compressed to a matter knot  $K$  at a massless limit.

## References

- [1] S. Cheng and P. Sułkowski, *3d  $N = 2$  theories and plumbing graphs: adding matter, gauging, and new dualities*, *JHEP* **08** (2023) 136, [[arXiv:2302.13371](#)].
- [2] K. A. Intriligator and N. Seiberg, *Mirror symmetry in three-dimensional gauge theories*, *Phys. Lett.* **B387** (1996) 513–519, [[hep-th/9607207](#)].
- [3] O. Aharony, A. Hanany, K. Intriligator, N. Seiberg, and M. J. Strassler, *Aspects of  $N=2$  Supersymmetric Gauge Theories in Three Dimensions*, *Nucl.Phys.B* **499** (1997) 67–99, [[hep-th/9703110](#)].

- [4] A. Hanany and E. Witten, *Type IIB superstrings, BPS monopoles, and three-dimensional gauge dynamics*, *Nucl.Phys.* **B492** (1997) 152–190, [[hep-th/9611230](#)].
- [5] A. Kapustin and M. J. Strassler, *On mirror symmetry in three-dimensional Abelian gauge theories*, *JHEP* **04** (1999) 021, [[hep-th/9902033](#)].
- [6] N. Dorey and D. Tong, *Mirror symmetry and toric geometry in three-dimensional gauge theories*, *JHEP* **05** (2000) 018, [[hep-th/9911094](#)].
- [7] A. Giveon and D. Kutasov, *Seiberg Duality in Chern-Simons Theory*, *Nucl. Phys. B* **812** (2009) 1–11, [[arXiv:0808.0360](#)].
- [8] F. Benini, C. Closset, and S. Cremonesi, *Comments on 3d seiberg-like dualities*, *JHEP* **1110** (2011) 075, [[arXiv:1108.5373](#)].
- [9] K. Intriligator and N. Seiberg, *Aspects of 3d  $N=2$  Chern-Simons-Matter Theories*, *JHEP* **07** (2013) 079, [[arXiv:1305.1633](#)].
- [10] L. F. Alday, P. Benetti Genolini, M. Bullimore, and M. van Loon, *Refined 3d-3d Correspondence*, *JHEP* **04** (2017) 170, [[arXiv:1702.05045](#)].
- [11] J. de Boer, K. Hori, Y. Oz, and Z. Yin, *Branes and Mirror Symmetry in  $N=2$  Supersymmetric Gauge Theories in Three Dimensions*, *Nucl.Phys.B* **502** (1997) 107–124, [[hep-th/9702154](#)].
- [12] S. Benvenuti and S. Pasquetti, *3d  $\mathcal{N} = 2$  mirror symmetry, pq-webs and monopole superpotentials*, *JHEP* **08** (2016) 136, [[arXiv:1605.02675](#)].
- [13] S. Cheng, *3d  $\mathcal{N} = 2$  brane webs and quiver matrices*, *JHEP* **07** (2022) 107, [[arXiv:2108.03696](#)].
- [14] T. Dimofte, D. Gaiotto, and S. Gukov, *Gauge Theories Labelled by Three-Manifolds*, *Commun. Math. Phys.* **325** (2014) 367–419, [[arXiv:1108.4389](#)].
- [15] S. Gukov, P. Putrov, and C. Vafa, *Fivebranes and 3-manifold homology*, *JHEP* **07** (2017) 071, [[arXiv:1602.05302](#)].
- [16] S. Cecotti, C. Cordova, and C. Vafa, *Braids, Walls, and Mirrors*, [arXiv:1110.2115](#).
- [17] Y. Terashima and M. Yamazaki,  *$SL(2, R)$  Chern-Simons, Liouville, and Gauge Theory on Duality Walls*, *JHEP* **08** (2011) 135, [[arXiv:1103.5748](#)].
- [18] S. Gukov, D. Pei, P. Putrov, and C. Vafa, *BPS spectra and 3-manifold invariants*, *J. Knot Theor. Ramifications* **29** (2020), no. 02 2040003, [[arXiv:1701.06567](#)].
- [19] M. C. N. Cheng, S. Chun, F. Ferrari, S. Gukov, and S. M. Harrison, *3d modularity*, *JHEP* **10** (2019) 010, [[arXiv:1809.10148](#)].
- [20] A. Gadde, S. Gukov, and P. Putrov, *Fivebranes and 4-manifolds*, *Prog. Math.* **319** (2016) 155–245, [[arXiv:1306.4320](#)].
- [21] R. Kirby, *A Calculus for Framed Links in  $S^3$* , *Inventiones mathematicae* **45** (1978) 35–56.
- [22] H. Ooguri and C. Vafa, *Knot invariants and topological strings*, *Nucl. Phys.* **B577** (2000) 419–438, [[hep-th/9912123](#)].
- [23] S. Cheng, *Mirror symmetry and mixed Chern-Simons levels for Abelian 3D  $N=2$  theories*, *Phys. Rev. D* **104** (2021), no. 4 046011, [[arXiv:2010.15074](#)].
- [24] E. Witten,  *$SL(2, Z)$  action on three-dimensional conformal field theories with Abelian symmetry*, [hep-th/0307041](#).

- [25] J. Eckhard, H. Kim, S. Schafer-Nameki, and B. Willett, *Higher-form symmetries, beth vacua, and the 3d-3d correspondence*, *JHEP* **01** (2020) 101, [[arXiv:1910.14086](#)].
- [26] L. Bhardwaj, M. Bullimore, A. E. V. Ferrari, and S. Schafer-Nameki, *Anomalies of Generalized Symmetries from Solitonic Defects*, [arXiv:2205.15330](#).
- [27] F. Benini, C. Closset, and S. Cremonesi, *Quantum moduli space of Chern-Simons quivers, wrapped D6-branes and AdS<sub>4</sub>/CFT<sub>3</sub>*, *JHEP* **09** (2011) 005, [[arXiv:1105.2299](#)].
- [28] M. Sacchi, O. Sela, and G. Zafrir, *Compactifying 5d superconformal field theories to 3d*, *JHEP* **09** (2021) 149, [[arXiv:2105.01497](#)].
- [29] C. Hwang, S. Pasquetti, and M. Sacchi, *Rethinking mirror symmetry as a local duality on fields*, *Phys. Rev. D* **106** (2022), no. 10 105014, [[arXiv:2110.11362](#)].
- [30] M. Najjar, J. Tian and Y. N. Wang, *3d  $\mathcal{N} = 2$  theories from M-theory on CY<sub>4</sub> and IIB brane box*, *JHEP* **05** (2024) 038, [[arXiv:2312.17082](#)].
- [31] T. Kitao, K. Ohta, and N. Ohta, *Three-dimensional gauge dynamics from brane configurations with (p,q)-fivebrane*, *Nucl.Phys.* **B539** (1999) 79–106, [[hep-th/9808111](#)].
- [32] T. Dimofte, S. Gukov, and L. Hollands, *Vortex Counting and Lagrangian 3-manifolds*, *Lett. Math. Phys.* **98** (2011) 225–287, [[arXiv:1006.0977](#)].
- [33] S. Gukov and D. Pei, *Equivariant Verlinde formula from fivebranes and vortices*, *Commun. Math. Phys.* **355** (2017), no. 1 1–50, [[arXiv:1501.01310](#)].
- [34] H.-J. Chung, T. Dimofte, S. Gukov, and P. Sułkowski, *3d-3d correspondence revisited*, *JHEP* **1604** (2016) 140, [[arXiv:1405.3663](#)].
- [35] S. Cheng and P. Sułkowski, *Refined open topological strings revisited*, *Phys. Rev. D* **104** (2021), no. 10 106012, [[arXiv:2104.00713](#)].
- [36] D. Gaiotto and E. Witten, *S-Duality of Boundary Conditions In N=4 Super Yang-Mills Theory*, *Adv. Theor. Math. Phys.* **13** (2009), no. 3 721–896, [[arXiv:0807.3720](#)].
- [37] D. Tong, *Gauge Theory*. <http://www.damtp.cam.ac.uk/user/tong/gaugetheory.html>, 2018.
- [38] D. Rolfsen, *Rational surgery calculus:extension of Kirby’s theorem*, *Pacific Journal of Mathematics* **110** (1984), no. 2 377–386.
- [39] T. Dimofte, D. Gaiotto, and R. van der Veen, *RG Domain Walls and Hybrid Triangulations*, *Adv. Theor. Math. Phys.* **19** (2015) 137–276, [[arXiv:1304.6721](#)].
- [40] D. Rolfsen, *Knots and links*, vol. 346. American Mathematical Society, 1976.
- [41] D. Gang, N. Kim, M. Romo, and M. Yamazaki, *Aspects of defects in 3d-3d correspondence*, *JHEP* **10** (2016) 062, [[arXiv:1510.05011](#)].
- [42] E. Witten, *Quantum field theory and the Jones polynomial*, *Commun. Math. Phys.* **121** (1989), no. 351-399.
- [43] V. Prasolov and A. Sossinsky, *Knots, Links, Braids and 3-Manifolds*, vol. 154. American Mathematical Society, 1997.
- [44] P. Kucharski, M. Reineke, M. Stosic, and P. Sułkowski, *BPS states, knots and quivers*, *Phys. Rev.* **D96** (2017), no. 12 121902, [[arXiv:1707.02991](#)].
- [45] P. Kucharski, M. Reineke, M. Stosic, and P. Sułkowski, *Knots-quivers correspondence*, *Adv. Theor. Math. Phys.* **23** (2019) 1849–1902, [[arXiv:1707.04017](#)].

- [46] Q. Chen and T. Yang, *Volume conjectures for the Reshetikhin–Turaev and the Turaev–Viro invariants*, *Quantum Topol.* **9** (2018), no. 3 419–460, [[arXiv:1503.02547](#)].
- [47] R. Gopakumar and C. Vafa, *On the gauge theory / geometry correspondence*, *Adv. Theor. Math. Phys.* **3** (1999) 1415–1443, [[hep-th/9811131](#)].
- [48] J. M. F. Labastida, M. Marino, and C. Vafa, *Knots, links and branes at large  $N$* , *JHEP* **11** (2000) 007, [[hep-th/0010102](#)].